The physics potential of future parity violation experiments

Frank Petriello

Northwestern University

Argonne NATIONAL LABORATORY

2023 Summer Hall A/C Meeting

July 30, 2023

Outline

- This talk will focus on the new physics potential of planned future parity violation experiments.
- Often searches for high-scale new physics are considered the provenance of the LHC.
- We will see that there are many holes in the LHC coverage where new physics could be missed, and that the ability to polarize beams at future experiments such as SoLID and the EIC complements the LHC program.
- Topics we will survey:
  - Motivation, and review of the Standard Model Effective Field Theory (SMEFT), the framework we will use for model-independent new physics searches
  - Polarization asymmetry measurements in PVDIS at a future EIC and new physics searches
  - Low-energy probes of new physics at P2 and SoLID
  - Transverse spin asymmetries and anomalous dipole moments at the EIC

Status of the Standard Model

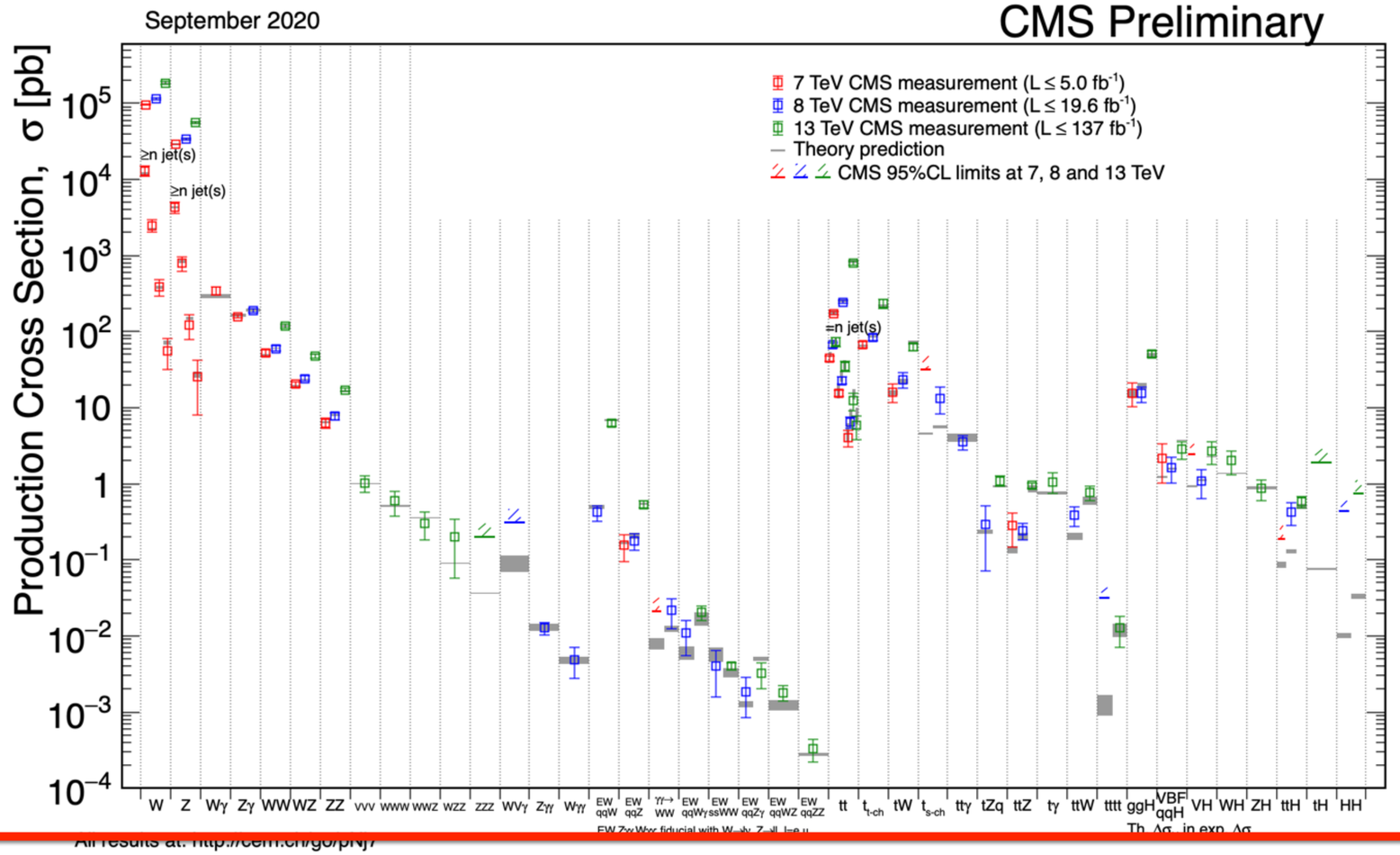

Remarkable agreement between SM theory and experiment over dozens of processes and orders of magnitude in cross section. No BSM deviation found so far!

Resonance searches

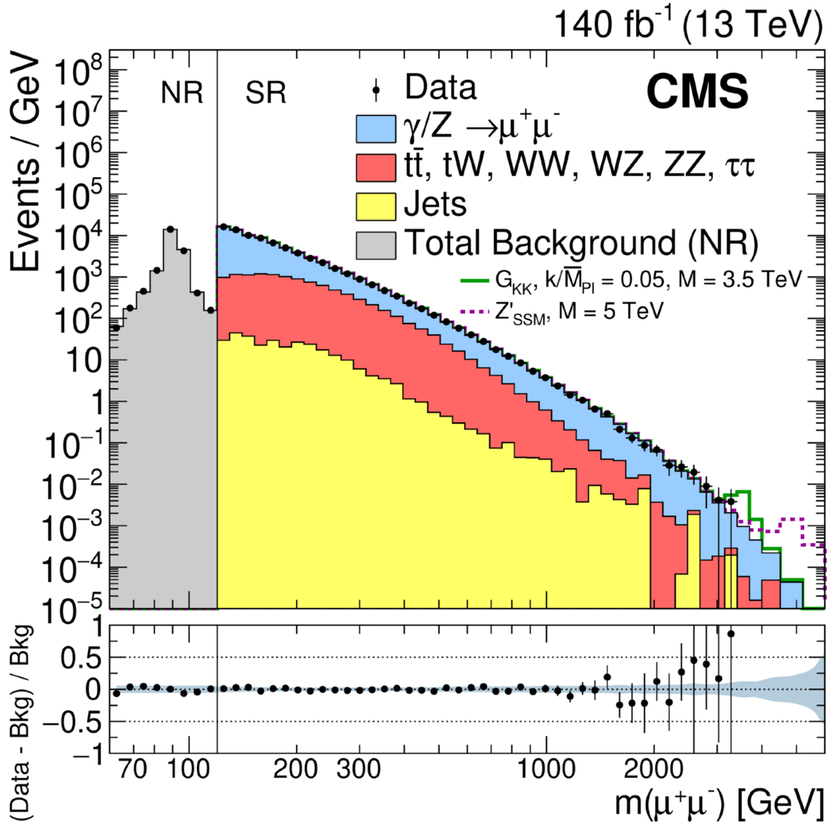

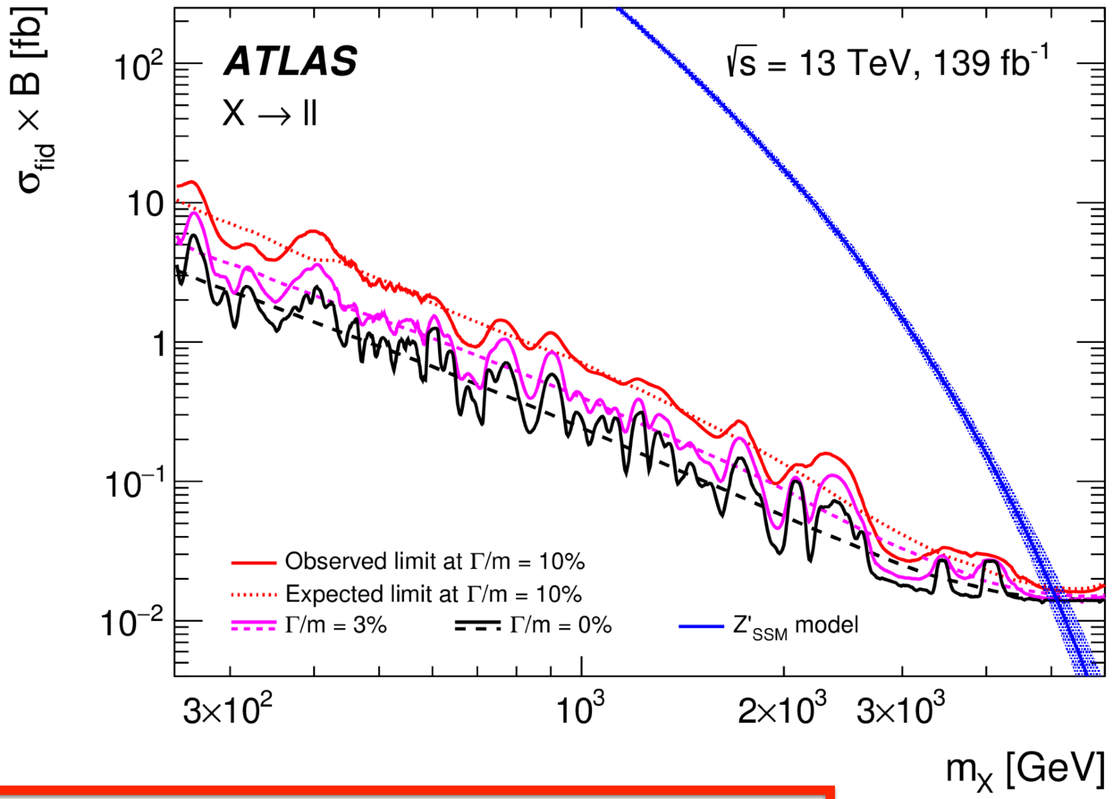

Sensitivity to new resonances has reached 5 TeV in some models. Suggests a mass gap between SM and new physics; indirect searches increasingly important

EFT frameworks for new physics searches

- The Standard Model Effective Field Theory is an EFT framework that encapsulates both the lack of new particles beyond the SM, and a mass gap between the SM and any new states. It provides a well-defined framework for current and future studies.

Λ≫vev, E

$$\mathcal{L} = \mathcal{L}_{SM} + \frac{1}{\Lambda^2}\sum_i C_{6,i}\mathcal{O}_{6,i} + \frac{1}{\Lambda^4}\sum_i C_{8,i}\mathcal{O}_{8,i}$$

Dimension-6 **Dimension-8**

The theory contains all operators consistent with the SM gauge symmetries. It is a consistent and predictive QFT: it is renormalizable order-by-order in Λ. The Wilson coefficients C_i depend on the parameters of the underlying UV model.

What the SMEFT is designed to handle:

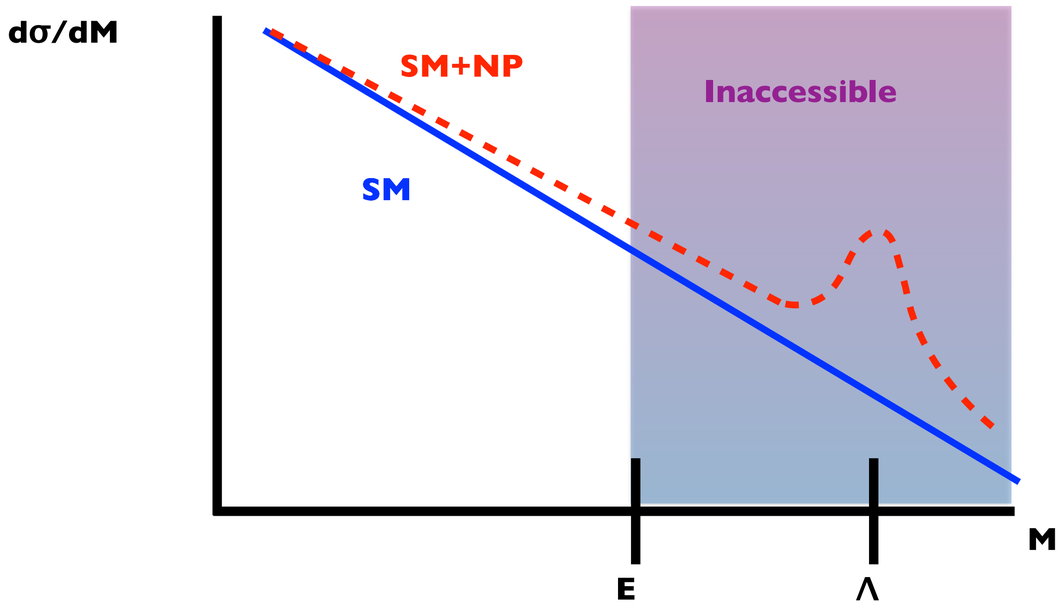

EFT frameworks for new physics searches

- The development of the SMEFT as a fully consistent QFT ready for comparison with experiment, with higher-order corrections and renormalization-group effects incorporated, has been a great success of the past decade.

Pure Gauge interactions

Accommodates a rich phenomenology in all sectors

X^3	
Q_G	$f^{ABC}G^{A\nu}_{\mu}G^{B\rho}_{\nu}G^{C\mu}_{\rho}$
$Q_{\widetilde{G}}$	$f^{ABC}\widetilde{G}^{A\nu}_{\mu}G^{B\rho}_{\nu}G^{C\mu}_{\rho}$
Q_W	$\varepsilon^{IJK}W^{I\nu}_{\mu}W^{J\rho}_{\nu}W^{K\mu}_{\rho}$
$Q_{\widetilde{W}}$	$\varepsilon^{IJK}\widetilde{W}^{I\nu}_{\mu}W^{J\rho}_{\nu}W^{K\mu}_{\rho}$

φ^6 and $\varphi^4 D^2$	
Q_{φ}	$(\varphi^\dagger\varphi)^3$
$Q_{\varphi\Box}$	$(\varphi^\dagger\varphi)\Box(\varphi^\dagger\varphi)$
$Q_{\varphi D}$	$\left(\varphi^\dagger D^\mu\varphi\right)^*\left(\varphi^\dagger D_\mu\varphi\right)$

$\psi^2\varphi^3$	
$Q_{e\varphi}$	$(\varphi^\dagger\varphi)(\bar{l}_p e_r\varphi)$
$Q_{u\varphi}$	$(\varphi^\dagger\varphi)(\bar{q}_p u_r\widetilde{\varphi})$
$Q_{d\varphi}$	$(\varphi^\dagger\varphi)(\bar{q}_p d_r\varphi)$

$X^2\varphi^2$	
$Q_{\varphi G}$	$\varphi^\dagger\varphi\, G^A_{\mu\nu}G^{A\mu\nu}$
$Q_{\varphi\widetilde{G}}$	$\varphi^\dagger\varphi\, \widetilde{G}^A_{\mu\nu}G^{A\mu\nu}$
$Q_{\varphi W}$	$\varphi^\dagger\varphi\, W^I_{\mu\nu}W^{I\mu\nu}$
$Q_{\varphi\widetilde{W}}$	$\varphi^\dagger\varphi\, \widetilde{W}^I_{\mu\nu}W^{I\mu\nu}$
$Q_{\varphi B}$	$\varphi^\dagger\varphi\, B_{\mu\nu}B^{\mu\nu}$
$Q_{\varphi\widetilde{B}}$	$\varphi^\dagger\varphi\, \widetilde{B}_{\mu\nu}B^{\mu\nu}$
$Q_{\varphi WB}$	$\varphi^\dagger\tau^I\varphi\, W^I_{\mu\nu}B^{\mu\nu}$
$Q_{\varphi\widetilde{W}B}$	$\varphi^\dagger\tau^I\varphi\, \widetilde{W}^I_{\mu\nu}B^{\mu\nu}$

$\psi^2 X\varphi$	
Q_{eW}	$(\bar{l}_p\sigma^{\mu\nu}e_r)\tau^I\varphi W^I_{\mu\nu}$
Q_{eB}	$(\bar{l}_p\sigma^{\mu\nu}e_r)\varphi B_{\mu\nu}$
Q_{uG}	$(\bar{q}_p\sigma^{\mu\nu}T^A u_r)\widetilde{\varphi}\, G^A_{\mu\nu}$
Q_{uW}	$(\bar{q}_p\sigma^{\mu\nu}u_r)\tau^I\widetilde{\varphi}\, W^I_{\mu\nu}$
Q_{uB}	$(\bar{q}_p\sigma^{\mu\nu}u_r)\widetilde{\varphi}\, B_{\mu\nu}$
Q_{dG}	$(\bar{q}_p\sigma^{\mu\nu}T^A d_r)\varphi\, G^A_{\mu\nu}$
Q_{dW}	$(\bar{q}_p\sigma^{\mu\nu}d_r)\tau^I\varphi\, W^I_{\mu\nu}$
Q_{dB}	$(\bar{q}_p\sigma^{\mu\nu}d_r)\varphi\, B_{\mu\nu}$

$\psi^2\varphi^2 D$	
$Q^{(1)}_{\varphi l}$	$(\varphi^\dagger i\overleftrightarrow{D}_\mu\varphi)(\bar{l}_p\gamma^\mu l_r)$
$Q^{(3)}_{\varphi l}$	$(\varphi^\dagger i\overleftrightarrow{D}^I_\mu\varphi)(\bar{l}_p\tau^I\gamma^\mu l_r)$
$Q_{\varphi e}$	$(\varphi^\dagger i\overleftrightarrow{D}_\mu\varphi)(\bar{e}_p\gamma^\mu e_r)$
$Q^{(1)}_{\varphi q}$	$(\varphi^\dagger i\overleftrightarrow{D}_\mu\varphi)(\bar{q}_p\gamma^\mu q_r)$
$Q^{(3)}_{\varphi q}$	$(\varphi^\dagger i\overleftrightarrow{D}^I_\mu\varphi)(\bar{q}_p\tau^I\gamma^\mu q_r)$
$Q_{\varphi u}$	$(\varphi^\dagger i\overleftrightarrow{D}_\mu\varphi)(\bar{u}_p\gamma^\mu u_r)$
$Q_{\varphi d}$	$(\varphi^\dagger i\overleftrightarrow{D}_\mu\varphi)(\bar{d}_p\gamma^\mu d_r)$
$Q_{\varphi ud}$	$i(\widetilde{\varphi}^\dagger D_\mu\varphi)(\bar{u}_p\gamma^\mu d_r)$

$(\bar{L}L)(\bar{L}L)$	
Q_{ll}	$(\bar{l}_p\gamma_\mu l_r)(\bar{l}_s\gamma^\mu l_t)$
$Q^{(1)}_{qq}$	$(\bar{q}_p\gamma_\mu q_r)(\bar{q}_s\gamma^\mu q_t)$
$Q^{(3)}_{qq}$	$(\bar{q}_p\gamma_\mu\tau^I q_r)(\bar{q}_s\gamma^\mu\tau^I q_t)$
$Q^{(1)}_{lq}$	$(\bar{l}_p\gamma_\mu l_r)(\bar{q}_s\gamma^\mu q_t)$
$Q^{(3)}_{lq}$	$(\bar{l}_p\gamma_\mu\tau^I l_r)(\bar{q}_s\gamma^\mu\tau^I q_t)$

$(\bar{R}R)(\bar{R}R)$	
Q_{ee}	$(\bar{e}_p\gamma_\mu e_r)(\bar{e}_s\gamma^\mu e_t)$
Q_{uu}	$(\bar{u}_p\gamma_\mu u_r)(\bar{u}_s\gamma^\mu u_t)$
Q_{dd}	$(\bar{d}_p\gamma_\mu d_r)(\bar{d}_s\gamma^\mu d_t)$
Q_{eu}	$(\bar{e}_p\gamma_\mu e_r)(\bar{u}_s\gamma^\mu u_t)$
Q_{ed}	$(\bar{e}_p\gamma_\mu e_r)(\bar{d}_s\gamma^\mu d_t)$
$Q^{(1)}_{ud}$	$(\bar{u}_p\gamma_\mu u_r)(\bar{d}_s\gamma^\mu d_t)$
$Q^{(8)}_{ud}$	$(\bar{u}_p\gamma_\mu T^A u_r)(\bar{d}_s\gamma^\mu T^A d_t)$

$(\bar{L}L)(\bar{R}R)$	
Q_{le}	$(\bar{l}_p\gamma_\mu l_r)(\bar{e}_s\gamma^\mu e_t)$
Q_{lu}	$(\bar{l}_p\gamma_\mu l_r)(\bar{u}_s\gamma^\mu u_t)$
Q_{ld}	$(\bar{l}_p\gamma_\mu l_r)(\bar{d}_s\gamma^\mu d_t)$
Q_{qe}	$(\bar{q}_p\gamma_\mu q_r)(\bar{e}_s\gamma^\mu e_t)$
$Q^{(1)}_{qu}$	$(\bar{q}_p\gamma_\mu q_r)(\bar{u}_s\gamma^\mu u_t)$
$Q^{(8)}_{qu}$	$(\bar{q}_p\gamma_\mu T^A q_r)(\bar{u}_s\gamma^\mu T^A u_t)$
$Q^{(1)}_{qd}$	$(\bar{q}_p\gamma_\mu q_r)(\bar{d}_s\gamma^\mu d_t)$
$Q^{(8)}_{qd}$	$(\bar{q}_p\gamma_\mu T^A q_r)(\bar{d}_s\gamma^\mu T^A d_t)$

$(\bar{L}R)(\bar{R}L)$ and $(\bar{L}R)(\bar{L}R)$	
Q_{ledq}	$(\bar{l}^j_p e_r)(\bar{d}_s q^j_t)$
$Q^{(1)}_{quqd}$	$(\bar{q}^j_p u_r)\varepsilon_{jk}(\bar{q}^k_s d_t)$
$Q^{(8)}_{quqd}$	$(\bar{q}^j_p T^A u_r)\varepsilon_{jk}(\bar{q}^k_s T^A d_t)$
$Q^{(1)}_{lequ}$	$(\bar{l}^j_p e_r)\varepsilon_{jk}(\bar{q}^k_s u_t)$
$Q^{(3)}_{lequ}$	$(\bar{l}^j_p\sigma_{\mu\nu}e_r)\varepsilon_{jk}(\bar{q}^k_s\sigma^{\mu\nu}u_t)$

B-violating	
Q_{duq}	$\varepsilon^{\alpha\beta\gamma}\varepsilon_{jk}\left[(d^\alpha_p)^T C u^\beta_r\right]\left[(q^{\gamma j}_s)^T C l^k_t\right]$
Q_{qqu}	$\varepsilon^{\alpha\beta\gamma}\varepsilon_{jk}\left[(q^{\alpha j}_p)^T C q^{\beta k}_r\right]\left[(u^\gamma_s)^T C e_t\right]$
Q_{qqq}	$\varepsilon^{\alpha\beta\gamma}\varepsilon_{jn}\varepsilon_{km}\left[(q^{\alpha j}_p)^T C q^{\beta k}_r\right]\left[(q^{\gamma m}_s)^T C l^n_t\right]$
Q_{duu}	$\varepsilon^{\alpha\beta\gamma}\left[(d^\alpha_p)^T C u^\beta_r\right]\left[(u^\gamma_s)^T C e_t\right]$

Gauge-Higgs interactions

Fermion-Higgs-gauge interactions

Four-fermion interactions

Baryon-number violating interactions

Dimension-6 basis:

Buchmuller, Wyler (1986);
Grzadkowski et al (2010)

Dimension-6 RG running:

Alonso, Jenkins, Manojar, Trott (2013-2014)

Dimension-8 basis:

Murphy (2020)
Li et al (2020)

Matching explicit models to the EFT

- We can match explicit models to the EFT in a straightforward way. Each model leads to different patterns of Wilson coefficients. Measurements of the coefficients can help determine the underlying theory.

Example 1:

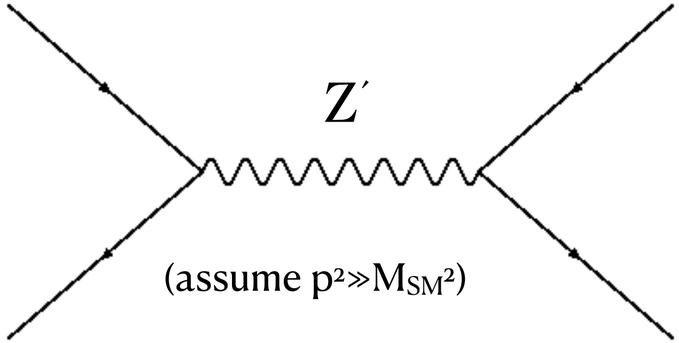

$$\sim -\frac{g_{Z'}^2}{p^2 - M_{Z'}^2} \approx \underbrace{\frac{g_{Z'}^2}{M_{Z'}^2}}_{\text{dim-6}} + \underbrace{\frac{g_{Z'}^2 p^2}{M_{Z'}^4}}_{\text{dim-8}} + \dots$$

$$\sigma \sim |\mathcal{M}_{SM}|^2 + \frac{1}{\Lambda^2} 2\mathrm{Re}\left[\mathcal{M}_6 \mathcal{M}_{SM}^*\right] + \frac{1}{\Lambda^4}\left\{|\mathcal{M}_6|^2 + 2\mathrm{Re}\left[\mathcal{M}_8 \mathcal{M}_{SM}^*\right]\right\}$$

$$\frac{g_{SM}^4}{p^4} \qquad \frac{g_{SM}^2 g_{Z'}^2}{p^2 M_{Z'}^2} \qquad \frac{g_{Z'}^4}{M_{Z'}^4} \qquad \frac{g_{SM}^2 g_{Z'}^2}{M_{Z'}^4}$$

Matching explicit models to the EFT

- We can match explicit models to the EFT in a straightforward way. Each model leads to different patterns of Wilson coefficients. Measurements of the coefficients can help determine the underlying theory.

Example 2:

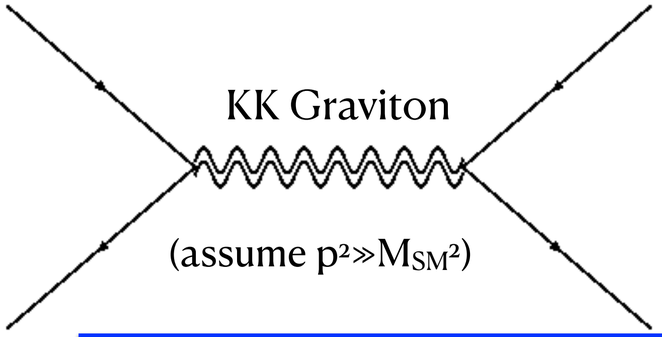

dim-6 dim-8

$$\sim 0 + \frac{p^2}{M_S^4} + \dots$$

Han, Lykken, Zhang (1998)

$$\sigma \sim |\mathcal{M}_{SM}|^2 + \frac{1}{\Lambda^2} 2\mathrm{Re}\left[\mathcal{M}_6 \mathcal{M}_{SM}^*\right] + \frac{1}{\Lambda^4}\left\{|\mathcal{M}_6|^2 + 2\mathrm{Re}\left[\mathcal{M}_8 \mathcal{M}_{SM}^*\right]\right\}$$

$$\frac{g_{SM}^4}{p^4} \qquad 0 \qquad 0 \qquad \frac{g_{SM}^2}{M_S^4}$$

Searching for deviations

- The most natural experiments to look for SMEFT-induced deviations are high-energy ones such as the LHC, since the expansion parameter E^2/Λ^2 is maximized there. Global fits to the available data are pursued by both the experimental and theoretical collaborations.

Ellis et al (2020)

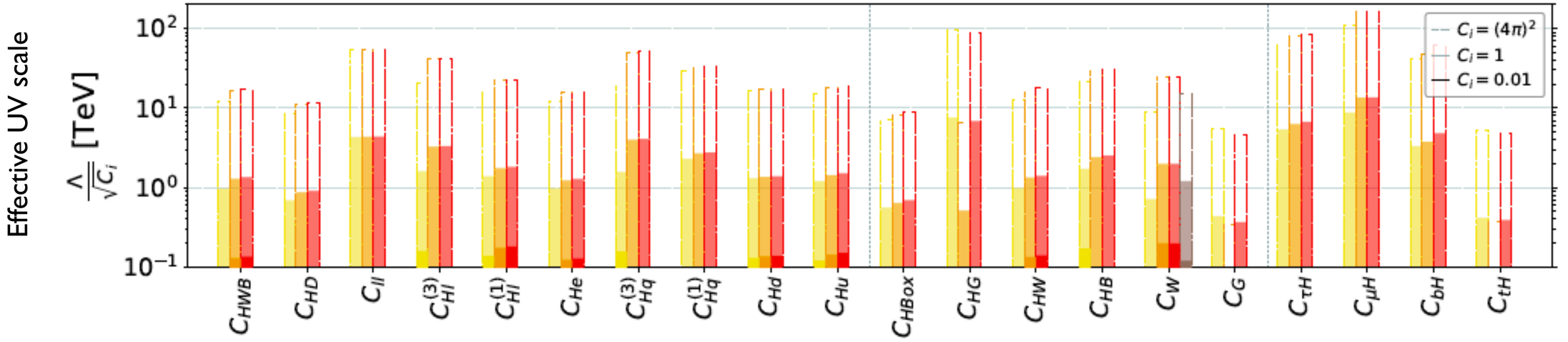

The LHC provides a rich program to search for a broad spectrum of coefficients to the TeV scale

Open question 1

- Given that different UV models can lead to very different patterns between dim-6 and dim-8 coefficients, we should make as few assumptions as possible regarding their relative size in SMEFT studies, and just let the data determine their allowed range. Despite the success of the LHC in pursuing this program there remain many open questions.

Have we identified a sufficiently broad set of observables to remove flat directions from SMEFT fits?

This is an example fit of two four-fermion operators to LHC Drell-Yan invariant mass data. One linear combination is strongly constrained, the other is not. Such flat directions appear often in LHC fits.

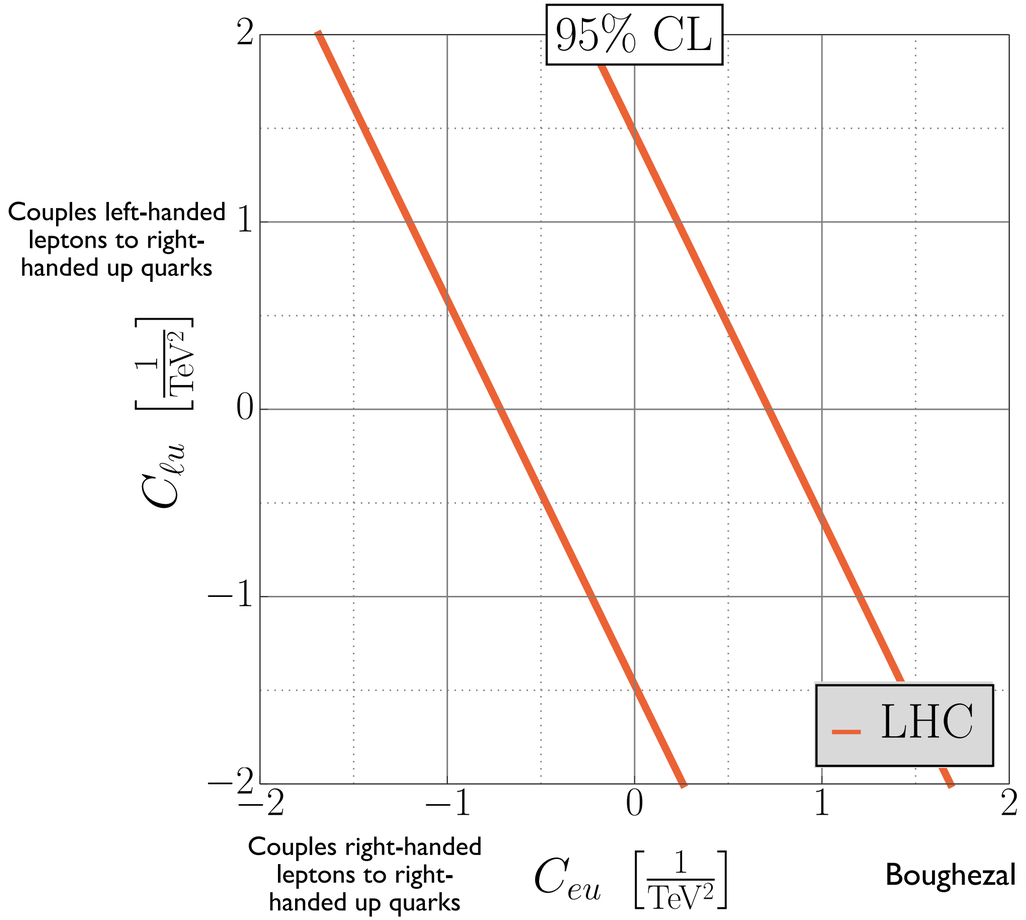

Boughezal et al (2022)

Open question 2

- Given that different UV models can lead to very different patterns between dim-6 and dim-8 coefficients, we should make as few assumptions as possible regarding their relative size in SMEFT studies, and just let the data determine their allowed range. Despite the success of the LHC in pursuing this program there remain many open questions.

Are dimension-8 effects important for the data sets we are considering, and can we separate them from dimension-6 effects?

Toy example:

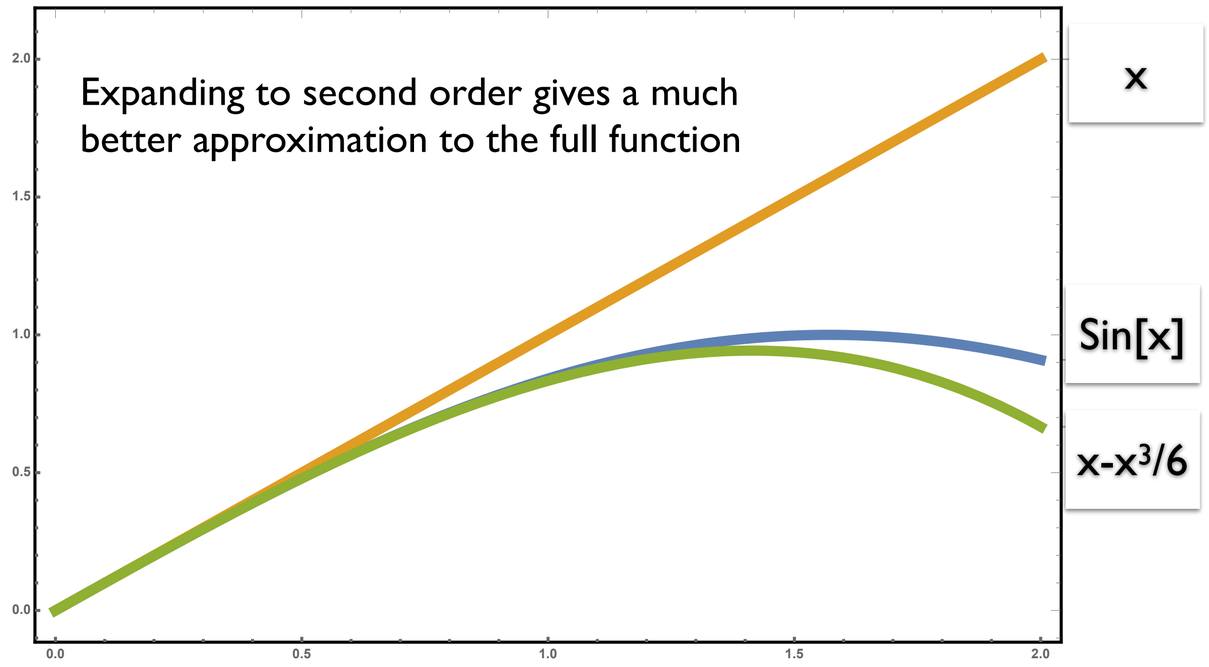

Open question 2

- Given that different UV models can lead to very different patterns between dim-6 and dim-8 coefficients, we should make as few assumptions as possible regarding their relative size in SMEFT studies, and just let the data determine their allowed range. Despite the success of the LHC in pursuing this program there remain many open questions.

Are dimension-8 effects important for the data sets we are considering, and can we separate them from dimension-6 effects?

This is again an LHC Drell-Yan example. Turning on dimension-8 coefficients widens the allowed range of dimension-6 by nearly a factor of 2, indicating the difficulty distinguishing between these effects.

Turn on only dim-6 correction

Turn on dim-6 and dim-8 corrections

	dim-6	single coupling	marginalized	marginalized*
C_{eu}	$[0.08, 1.0]$	$[0.1, 1.8]$	$[-39, 39]$	$[-0.6, 2.4]$
$C_{e^2u^2D^2}$	–	$[-1.5, 13]$	$[-17, 9.2 \cdot 10^3]$	$[-14, 18]$
$C_{e^2u^2H^2}$	–	$[45, 555]$	$[-1.9, 1.2] \cdot 10^4$	$[-256, 256]$
$C^{(1)-(2)}_{u^2H^2D^3}$	–	$[-24, -1.8] \cdot 10^3$	$[-1.2, 1.8] \cdot 10^5$	$[-256, 256]$

Boughezal, Mereghetti, FP (2021)

Dim-8 coefficients with same chirality structure, like what would appear when expanding a Z' model

Open question 3

- Given that different UV models can lead to very different patterns between dim-6 and dim-8 coefficients, we should make as few assumptions as possible regarding their relative size in SMEFT studies, and just let the data determine their allowed range. Despite the success of the LHC in pursuing this program there remain many open questions.

There are several exciting potential deviations between SM and experiment; can other experiments shed light on these?

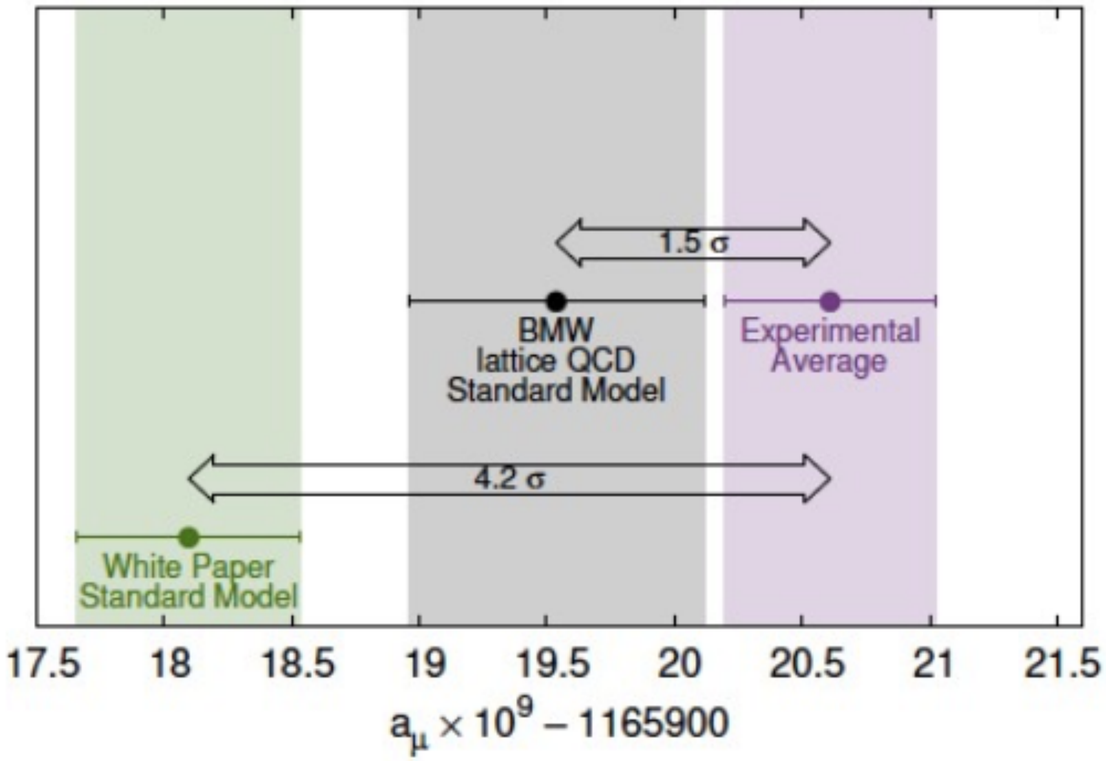

Open question 3

- Given that different UV models can lead to very different patterns between dim-6 and dim-8 coefficients, we should make as few assumptions as possible regarding their relative size in SMEFT studies, and just let the data determine their allowed range. Despite the success of the LHC in pursuing this program there remain many open questions.

There are several exciting potential deviations between SM and experiment; can other experiments shed light on these?

Most weakly constrainted dipole/ scalar operators at the LHC. , These effects are also sub-leading in the 1/Λ expansion and can be easily overwhelmed by the leading semi-leptonic, four-fermion operators

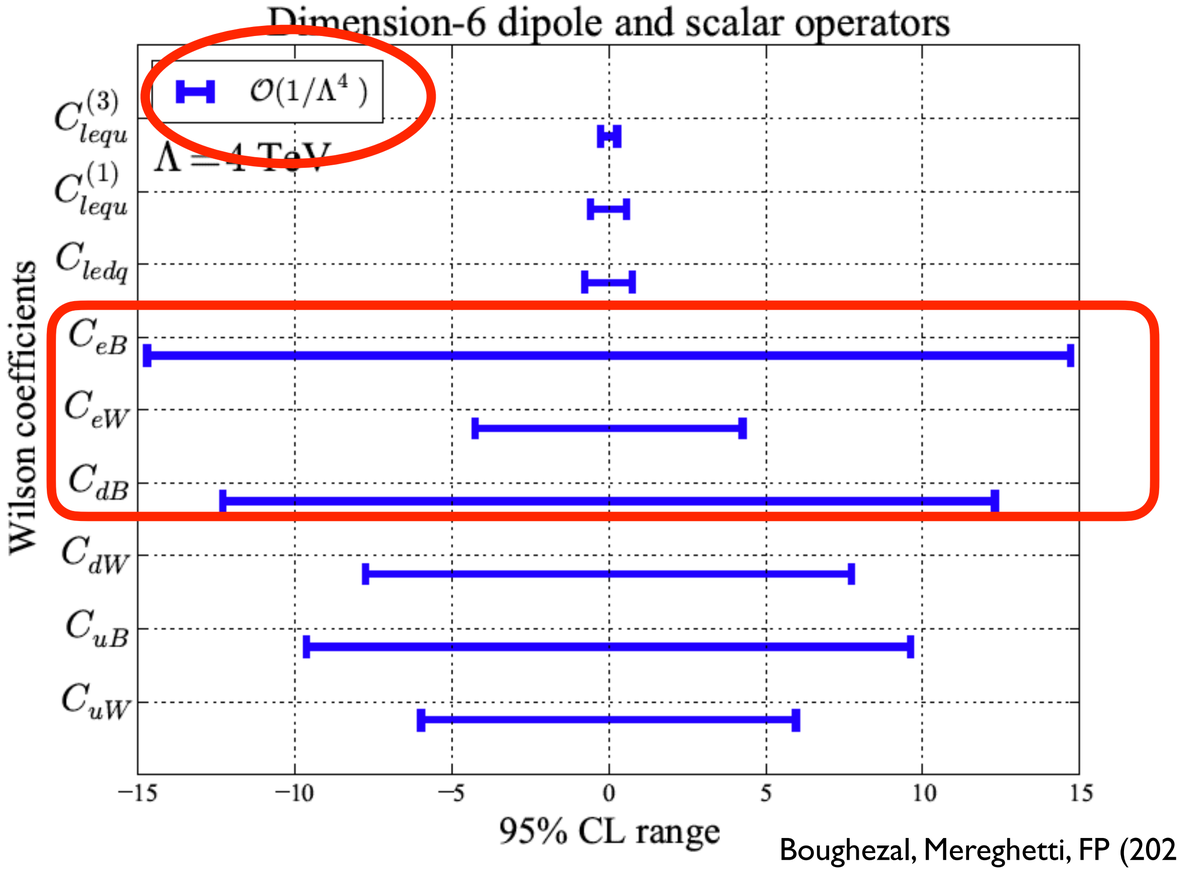

Boughezal, Mereghetti, FP (2021)

Open question 3

- Given that different UV models can lead to very different patterns between dim-6 and dim-8 coefficients, we should make as few assumptions as possible regarding their relative size in SMEFT studies, and just let the data determine their allowed range. Despite the success of the LHC in pursuing this program there remain many open questions.

There are s
potential deviat
and experim
experiments sh

We will show that PV measurements at future experiments play an important role in addressing all three issues

Most weakly constrainted dipole/ scalar operators at the LHC. , These effects are also sub-leading in the 1/Λ expansion and can be easily overwhelmed by the leading semi-leptonic, four-fermion operators

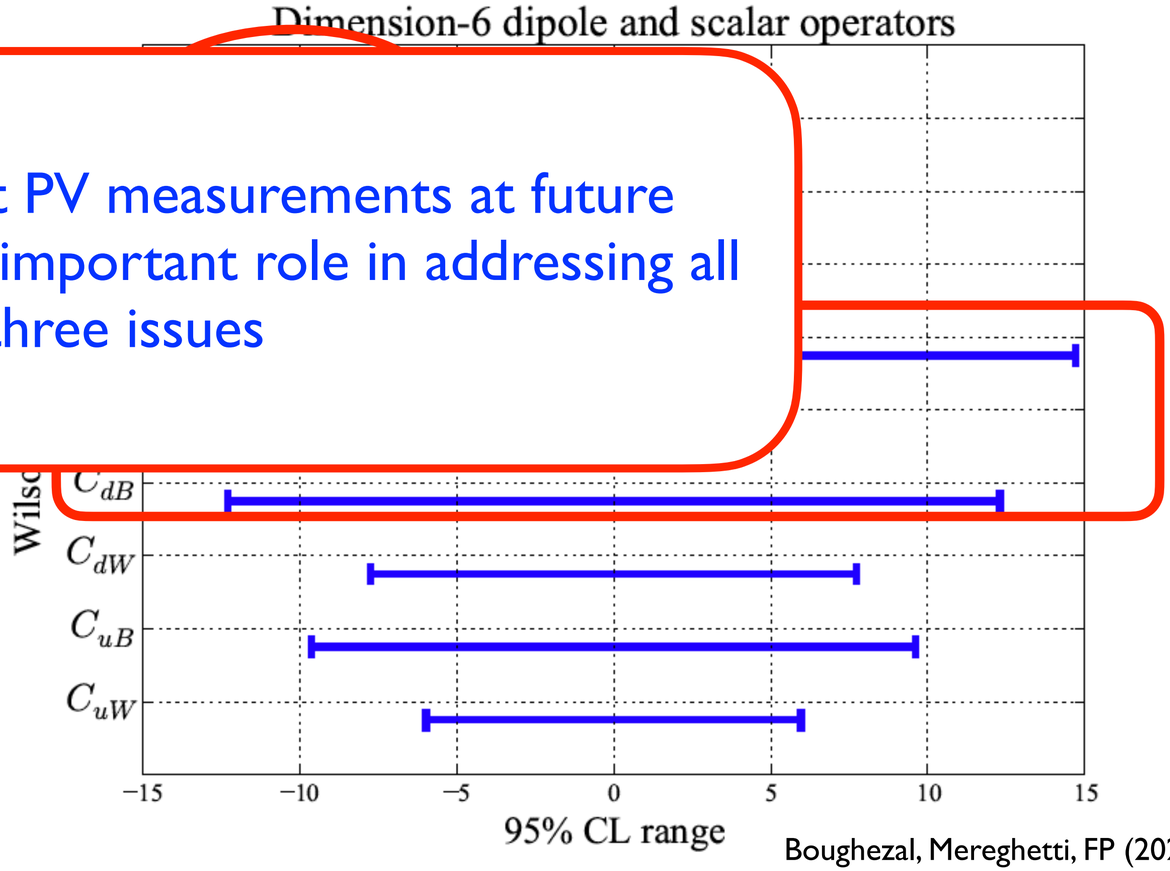

Boughezal, Mereghetti, FP (2021)

Polarization asymmetries at a future EIC

Boughezal, FP, Wiegand (2020)

Boughezal, Emmert, Kutz, Mantry, Nycz, FP, Simsek, Wiegand, Zheng (2022)

Semi-leptonic four-fermion operators

- We will begin by studying semi-leptonic four-fermion operators in the SMEFT. The natural place to search for them is through the Drell-Yan process at high energies.

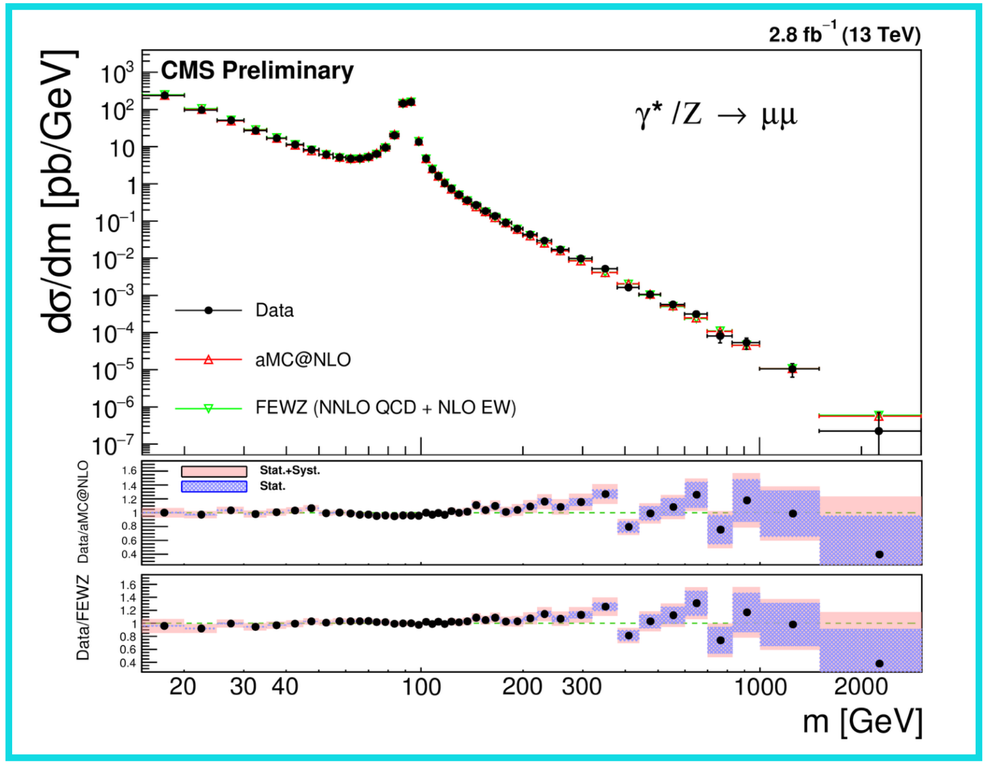

Both data and theory are precise up to high invariant masses

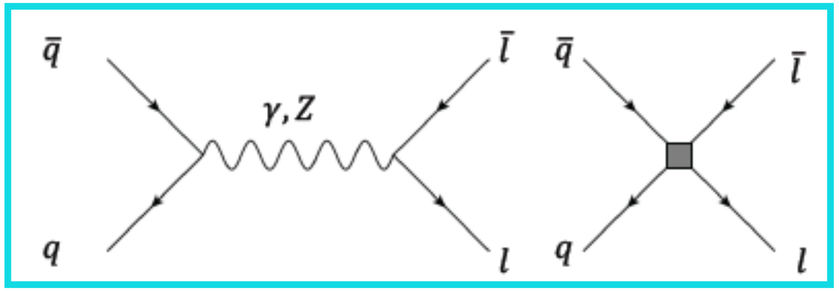

$\mathcal{O}_{lq}^{(1)}$	$(\bar{l}\gamma^\mu l)(\bar{q}\gamma_\mu q)$	$\mathcal{O}_{lu}$	$(\bar{l}\gamma^\mu l)(\bar{u}\gamma_\mu u)$
$\mathcal{O}_{lq}^{(3)}$	$(\bar{l}\gamma^\mu \tau^I l)(\bar{q}\gamma_\mu \tau^I q)$	$\mathcal{O}_{ld}$	$(\bar{l}\gamma^\mu l)(\bar{d}\gamma_\mu d)$
$\mathcal{O}_{eu}$	$(\bar{e}\gamma^\mu e)(\bar{u}\gamma_\mu u)$	$\mathcal{O}_{qe}$	$(\bar{q}\gamma^\mu q)(\bar{e}\gamma_\mu e)$
$\mathcal{O}_{ed}$	$(\bar{e}\gamma^\mu e)(\bar{d}\gamma_\mu d)$		

At the dimension-6 level there are 7 important operators

q,l are left-handed doublets; e,u,d are right-handed singlets

Blind spots in model space

- The structure of the matrix elements, and the limited numbers of observables that are measured in high-energy Drell-Yan (primarily invariant mass distributions) lead to degeneracies in fits to Wilson coefficients. This is seen in explicit fits to the data, and indicates that the LHC has blind spots in model space.

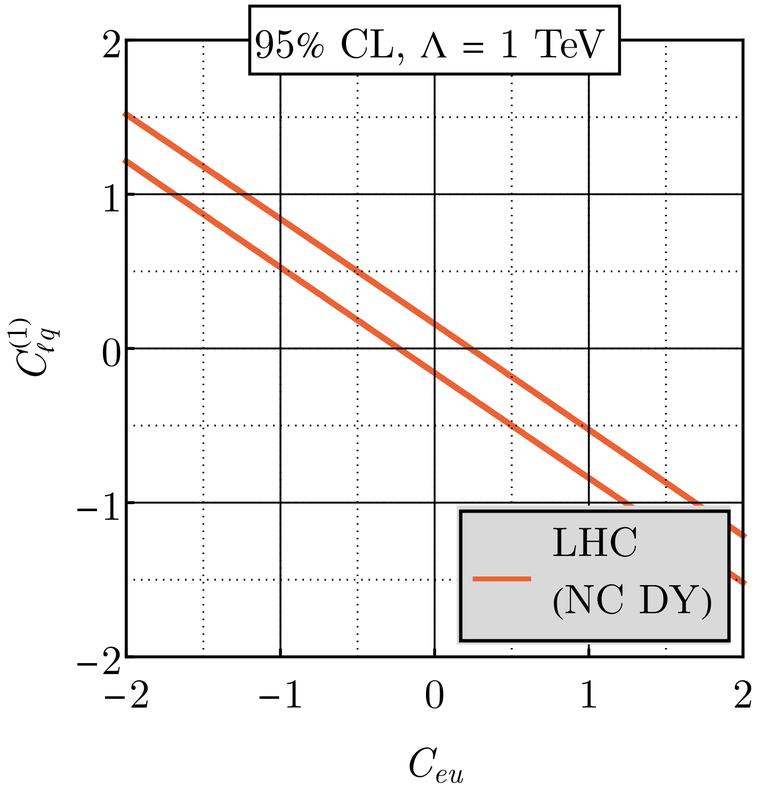

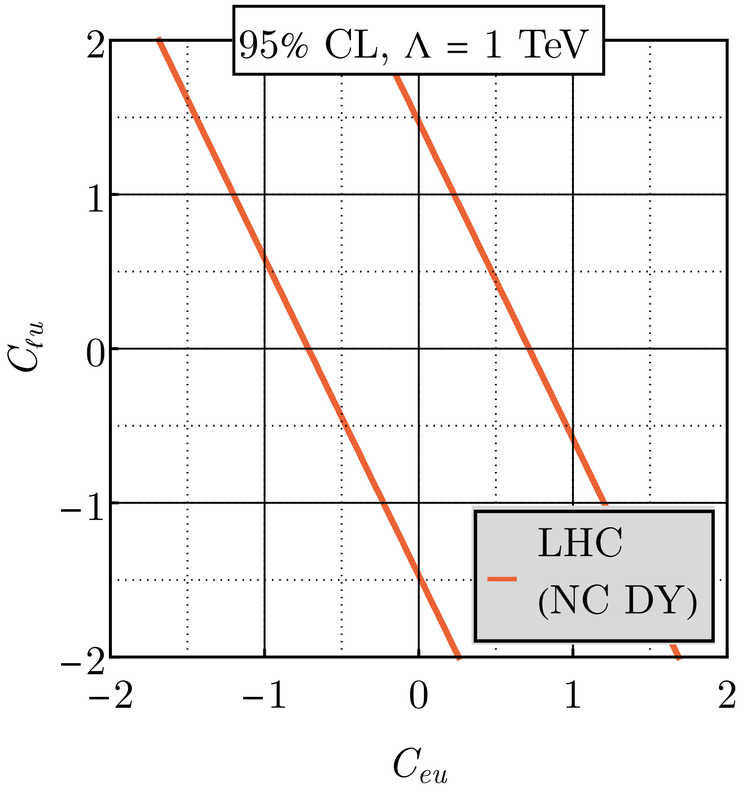

Boughezal, FP Wiegand (2020)

Asymmetries at the EIC

- We will consider several asymmetries that can be formed with planned EIC runs, and determine their sensitivity to SMEFT effects and the EIC complementarity with LHC probes.

- Polarized electrons, unpolarized hadrons:

$$A_{\rm PV} = \frac{{\rm d}\sigma_\ell}{{\rm d}\sigma_0}$$

- unpolarized electrons, polarized hadrons:

$$\Delta A_{\rm PV} = \frac{{\rm d}\sigma_H}{{\rm d}\sigma_0}$$

- lepton charge asymmetries:

$$A_{\rm LC} = \frac{{\rm d}\sigma_0(e^+H) - {\rm d}\sigma_0(e^-H)}{{\rm d}\sigma_0(e^+H) + {\rm d}\sigma_0(e^-H)}$$

(positron beam not part of the nominal EIC configuration, under discussion for future upgrades)

$$\begin{aligned}
{\rm d}\sigma_0 &= \frac{1}{4}\sum_q f_{q/H}[{\rm d}\sigma^{++} + {\rm d}\sigma^{+-} + {\rm d}\sigma^{-+} + {\rm d}\sigma^{--}] \\
{\rm d}\sigma_\ell &= \frac{1}{4}\sum_q f_{q/H}[{\rm d}\sigma^{++} + {\rm d}\sigma^{+-} - {\rm d}\sigma^{-+} - {\rm d}\sigma^{--}] \\
{\rm d}\sigma_H &= \frac{1}{4}\sum_q \Delta f_{q/H}[{\rm d}\sigma^{++} - {\rm d}\sigma^{+-} + {\rm d}\sigma^{-+} - {\rm d}\sigma^{--}]
\end{aligned}$$

Simulation details

- We generate EIC pseudodata for the following configurations that span the possible EIC beam configurations. The cuts, errors, and other parameters assumed are consistent with EIC expectations.

Deuteron		Proton	
D1	5 GeV × 41 GeV eD, 4.4 fb^{-1}	P1	5 GeV × 41 GeV ep, 4.4 fb^{-1}
D2	5 GeV × 100 GeV eD, 36.8 fb^{-1}	P2	5 GeV × 100 GeV ep, 36.8 fb^{-1}
D3	10 GeV × 100 GeV eD, 44.8 fb^{-1}	P3	10 GeV × 100 GeV ep, 44.8 fb^{-1}
D4	10 GeV × 137 GeV eD, 100 fb^{-1}	P4	10 GeV × 275 GeV ep, 100 fb^{-1}
D5	18 GeV × 137 GeV eD, 15.4 fb^{-1}	P5	18 GeV × 275 GeV ep, 15.4 fb^{-1}
		P6	18 GeV × 275 GeV ep, 100 fb^{-1}

- Red data sets provide the most sensitive probes of the SMEFT; we focus on these results in this talk. These are high luminosity/lower energy, and lower luminosity/high energy choices.
- Polarized deuteron and proton copies of these data sets are also studied, and labeled as ΔD, ΔP.
- We also consider a high-luminosity version of P5, D5, ΔP5, ΔD5 with x10 integrated luminosity.

1-d fit results

- We begin by turning on a single Wilson coefficient at a time. Choose C_{eu} as a representative example.

Bounds on the effective UV scale $\Lambda/\sqrt{C_{eu}}$

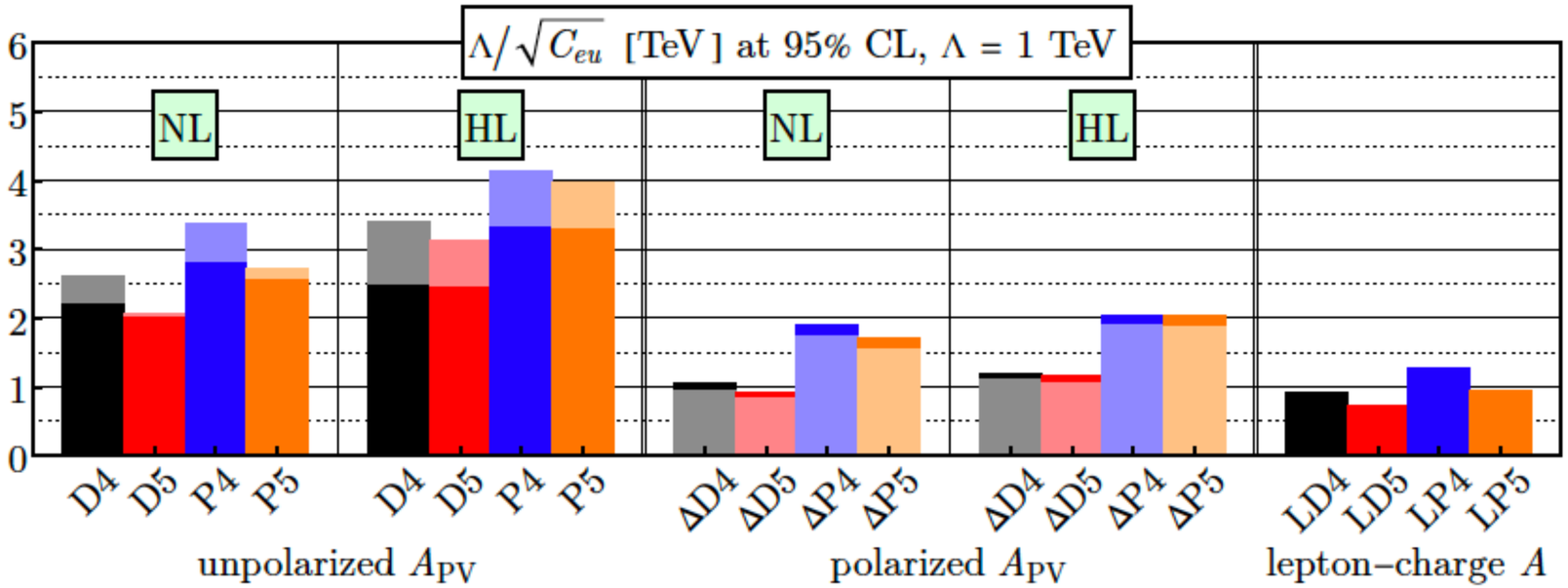

Trends:

- Proton sensitivities stronger than deuteron ones
- High luminosity, lower energy beats high energy, lower luminosity
- Unpolarized hadrons, polarized electrons offer strongest probes
- Lepton-charge asymmetries provide weakest probes

3 TeV scales probes with nominal luminosity, 4 TeV with high luminosity.
Competitive with current LHC bounds.

2-d fit results

- Most importantly, the EIC does not exhibit the blind spots that the LHC invariant mass data does. This is primarily due to it's ability to polarize beams and separate different helicity structures.

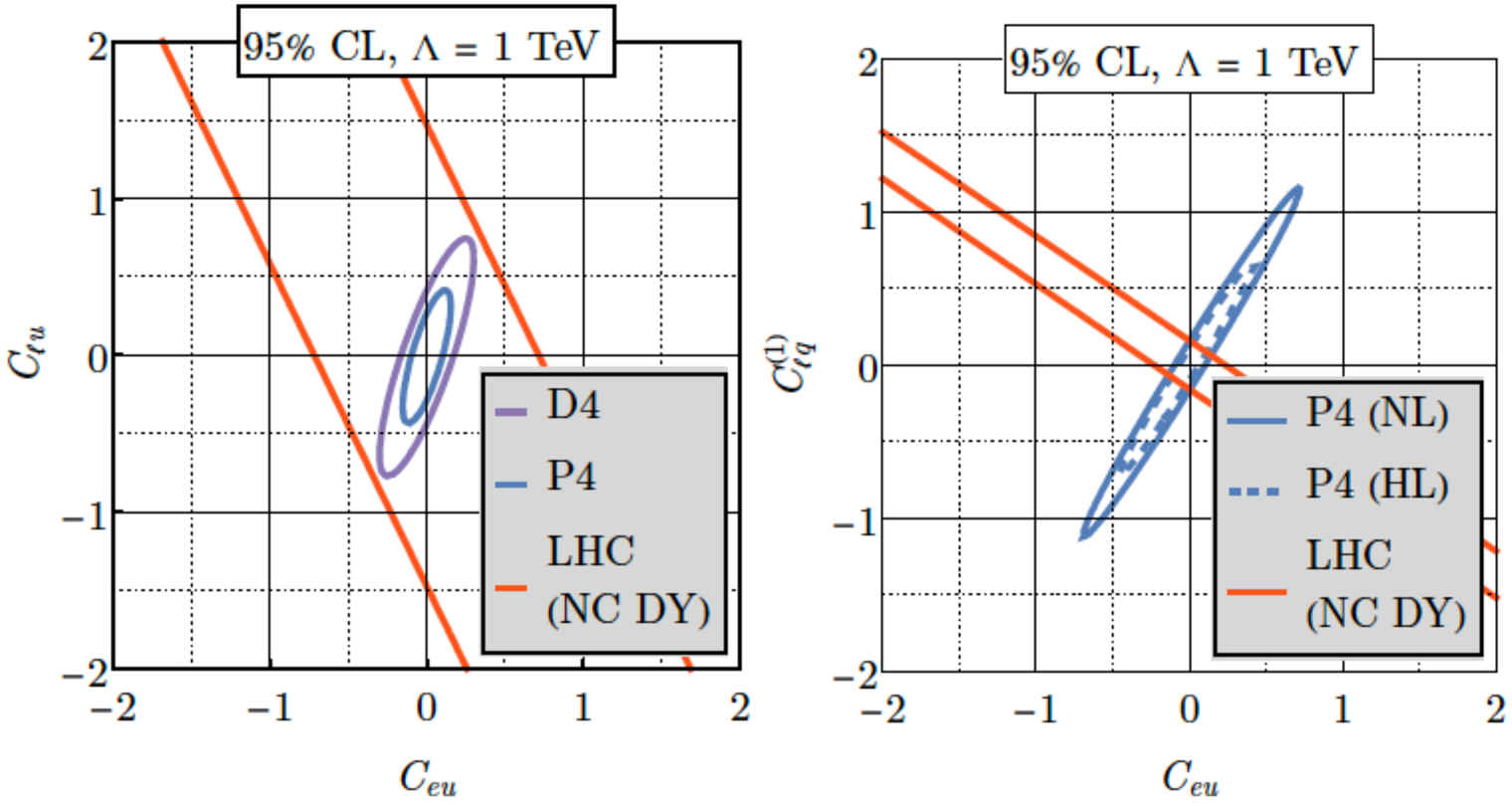

The EIC program nicely complements the LHC reach by closing off flat directions in the Wilson coefficient parameter space

Low-energy PVES/PVDIS probes of new physics

Boughezal, FP, Wiegand (2020)

Low-energy bounds

- High-intensity, low-energy experiments can probe very high energy scales and are often competitive with high energy measurements in searches for new physics. For example, Qweak probes semi-leptonic four-fermion operators at the several hundred GeV level for O(1) new physics couplings.

$(ee)(qq)$

	$[c_{\ell q}^{(3)}]_{1111}$	$[c_{\ell q}]_{1111}$	$[c_{\ell u}]_{1111}$	$[c_{\ell d}]_{1111}$	$[c_{eq}]_{1111}$	$[c_{eu}]_{1111}$	$[c_{ed}]_{1111}$
CHARM	-80 ± 180	700 ± 1800	370 ± 880	-700 ± 1800	x	x	x
APV	27 ± 19	$\mathbf{1.6 \pm 1.1}$	$\mathbf{3.4 \pm 2.3}$	$\mathbf{3.0 \pm 2.0}$	$\mathbf{-1.6 \pm 1.1}$	$\mathbf{-3.4 \pm 2.3}$	$\mathbf{-3.0 \pm 2.0}$
QWEAK	7.0 ± 12	-2.3 ± 4.0	-3.5 ± 6.0	-7 ± 12	2.3 ± 4.0	3.5 ± 6.0	7 ± 12
PVDIS	-8 ± 12	24 ± 35	38 ± 48	-77 ± 96	-77 ± 96	-12 ± 17	24 ± 35
SAMPLE	-8 ± 45	x	-17 ± 90	17 ± 90	x	-17 ± 90	17 ± 90
$d_j \to u\ell\nu$	$\mathbf{0.38 \pm 0.28}$	x	x	x	x	x	x
LEP-2	3.5 ± 2.2	-42 ± 28	-21 ± 14	42 ± 28	-18 ± 11	-9.0 ± 5.7	18 ± 11

$(\mu\mu)(qq)$

	$[c_{\ell q}^{(3)}]_{2211}$	$[c_{\ell q}]_{2211}$	$[c_{\ell u}]_{2211}$	$[c_{\ell d}]_{2211}$	$[c_{eq}]_{2211}$	$[c_{eu}]_{2211}$	$[c_{ed}]_{2211}$
PDG ν_μ	20 ± 15	$\mathbf{4 \pm 21}$	$\mathbf{18 \pm 19}$	$\mathbf{-20 \pm 37}$	x	x	x
SPS	0 ± 1000	0 ± 3000	0 ± 1500	0 ± 3000	$\mathbf{40 \pm 390}$	$\mathbf{-20 \pm 190}$	$\mathbf{40 \pm 390}$
$d_j \to u\ell\nu$	$\mathbf{-0.4 \pm 1.2}$	x	x	x	x	x	x

Note: operators are normalized according to C_i/v^2 where v is the Higgs vev.

Falkowski, Gonzalez-Alonso, Mimouni (2017)

Low-energy bounds

- Another important aspect of low-energy experiments is their ability to disentangle dimension-6 and dimension-8 Wilson coefficients in the EFT. Since the expansion parameter is E^2/Λ^2 these can leads to similar effects at high energies. In low-energy experiments the E^4/Λ^4 dimension-8 terms are completely negligible, and only dimension-6 is probed. We will study this in the semi-leptonic four-fermion sector, comparing upcoming low-energy experiments to Drell-Yan at the LHC.

Dimension 6		Dimension 8	
$\mathcal{O}_{lq}^{(1)}$	$\left(\bar{l}\gamma^\mu l\right)\left(\bar{q}\gamma_\mu q\right)$	$\mathcal{O}_{l^2q^2D^2}^{(1)}$	$D^\nu\left(\bar{l}\gamma^\mu l\right) D_\nu\left(\bar{q}\gamma_\mu q\right)$
$\mathcal{O}_{lq}^{(3)}$	$\left(\bar{l}\gamma^\mu \tau^i l\right)\left(\bar{q}\gamma_\mu \tau^i q\right)$	$\mathcal{O}_{l^2q^2D^2}^{(3)}$	$D^\nu\left(\bar{l}\gamma^\mu \tau^i l\right) D_\nu\left(\bar{q}\gamma_\mu \tau^i q\right)$
$\mathcal{O}_{eu}$	$\left(\bar{e}\gamma^\mu e\right)\left(\bar{u}\gamma_\mu u\right)$	$\mathcal{O}_{e^2u^2D^2}^{(1)}$	$D^\nu\left(\bar{e}\gamma^\mu e\right) D_\nu\left(\bar{u}\gamma_\mu u\right)$
$\mathcal{O}_{ed}$	$\left(\bar{e}\gamma^\mu e\right)\left(\bar{d}\gamma_\mu d\right)$	$\mathcal{O}_{e^2d^2D^2}^{(1)}$	$D^\nu\left(\bar{e}\gamma^\mu e\right) D_\nu\left(\bar{d}\gamma_\mu d\right)$
$\mathcal{O}_{lu}$	$\left(\bar{l}\gamma^\mu l\right)\left(\bar{u}\gamma_\mu u\right)$	$\mathcal{O}_{l^2u^2D^2}^{(1)}$	$D^\nu\left(\bar{l}\gamma^\mu l\right) D_\nu\left(\bar{u}\gamma_\mu u\right)$
$\mathcal{O}_{ld}$	$\left(\bar{l}\gamma^\mu l\right)\left(\bar{d}\gamma_\mu d\right)$	$\mathcal{O}_{l^2d^2D^2}^{(1)}$	$D^\nu\left(\bar{l}\gamma^\mu l\right) D_\nu\left(\bar{d}\gamma_\mu d\right)$
$\mathcal{O}_{qe}$	$\left(\bar{q}\gamma^\mu q\right)\left(\bar{e}\gamma_\mu e\right)$	$\mathcal{O}_{q^2e^2D^2}^{(1)}$	$D^\nu\left(\bar{q}\gamma^\mu q\right) D_\nu\left(\bar{e}\gamma_\mu e\right)$

Relevant operators for our analysis; note q,l are left-handed doublets; e,u,d are right-handed singlets

Basis choice

- In this talk we show results primarily in the SMEFT basis. But for the analysis of low-energy experiments we will also show results for a commonly-used basis for parity-violating experiments.

$$\begin{aligned}\mathcal{L}_{PV} = \frac{G_F}{\sqrt{2}}\Big[&(\overline{e}\gamma^\mu\gamma_5 e)(C^6_{1u}\overline{u}\gamma_\mu u + C^6_{1d}\overline{d}\gamma_\mu d) + (\overline{e}\gamma^\mu e)(C^6_{2u}\overline{u}\gamma_\mu\gamma_5 u + C^6_{2d}\overline{d}\gamma_\mu\gamma_5 d)\\ &+ (\overline{e}\gamma^\mu e)(C^6_{Vu}\overline{u}\gamma_\mu u + C^6_{Vd}\overline{d}\gamma_\mu d) + (\overline{e}\gamma^\mu\gamma_5 e)(C^6_{Au}\overline{u}\gamma_\mu\gamma_5 u)\\ &+ D^\nu\left(\overline{e}\gamma^\mu\gamma_5 e\right)D_\nu\left(\frac{C^8_{1u}}{v^2}\overline{u}\gamma_\mu u + \frac{C^8_{1d}}{v^2}\overline{d}\gamma_\mu d\right) + D^\nu\left(\overline{e}\gamma^\mu e\right)D_\nu\left(\frac{C^8_{2u}}{v^2}\overline{u}\gamma_\mu\gamma_5 u + \frac{C^8_{2d}}{v^2}\overline{d}\gamma_\mu\gamma_5 d\right)\\ &+ D^\nu\left(\overline{e}\gamma^\mu e\right)D_\nu\left(\frac{C^8_{Vu}}{v^2}\overline{u}\gamma_\mu u + \frac{C^8_{Vd}}{v^2}\overline{d}\gamma_\mu d\right) + D^\nu\left(\overline{e}\gamma^\mu\gamma_5 e\right)D_\nu\left(\frac{C^8_{Au}}{v^2}\overline{u}\gamma_\mu\gamma_5 u\right)\Big].\end{aligned}$$

SMEFT basis organizes the operators in terms of left and right-handed fields; the parity-violating basis uses vector and axial couplings

The coefficients in this expression are a sum of the SM contributions and new-physics SMEFT contributions:

$$C_i = C_i^{SM} + \Delta C_i^{NP}$$

We can derive a simple linear transformation between the two bases:

$$\begin{aligned}
C^6_{1u} &= \frac{v^2}{2\Lambda^2}\left\{-\left(C^{(1)}_{lq} - C^{(3)}_{lq}\right) + C_{eu} + C_{qe} - C_{lu}\right\}\\
C^6_{2u} &= \frac{v^2}{2\Lambda^2}\left\{-\left(C^{(1)}_{lq} - C^{(3)}_{lq}\right) + C_{eu} - C_{qe} + C_{lu}\right\}\\
C^6_{1d} &= \frac{v^2}{2\Lambda^2}\left\{-\left(C^{(1)}_{lq} + C^{(3)}_{lq}\right) + C_{ed} + C_{qe} - C_{ld}\right\}\\
C^6_{2d} &= \frac{v^2}{2\Lambda^2}\left\{-\left(C^{(1)}_{lq} + C^{(3)}_{lq}\right) + C_{ed} - C_{qe} + C_{ld}\right\}\\
C^6_{Vu} &= \frac{v^2}{2\Lambda^2}\left\{\left(C^{(1)}_{lq} - C^{(3)}_{lq}\right) + C_{eu} + C_{qe} + C_{lu}\right\}\\
C^6_{Au} &= \frac{v^2}{2\Lambda^2}\left\{\left(C^{(1)}_{lq} - C^{(3)}_{lq}\right) + C_{eu} - C_{qe} - C_{lu}\right\}\\
C^6_{Vd} &= \frac{v^2}{2\Lambda^2}\left\{\left(C^{(1)}_{lq} + C^{(3)}_{lq}\right) + C_{ed} + C_{qe} + C_{ld}\right\}.
\end{aligned}$$

Experiments considered and results

- We will consider two future low-energy PV experiments.

SoLID: deuteron target measurements used for BSM searches; sensitivity from region $0.4<x<0.5$, $Q^2\approx 6$ GeV^2. Total uncertainty, from both experiment and SM theory: 0.6%. Sensitive to both C_1 and C_2 coefficients in L_{PV}.

P2: following 1802.04759, projections includes Cesium APV, Qweak, SLAC constraints. Sensitive only to C_1 coefficients in L_{PV}; $2C_{1u}+C_{1d}$ (hydrogen target), $C_{1u}+C_{1d}$ (carbon target)

Comments:

- Note the elongated LHC ellipse; degeneracy in the Drell-Yan matrix elements; occurs at high m_{ll} where BSM effects are largest
- P2 sensitive only to C_1 coefficients
- Important contributions from SoLID; constraints orthogonal to LHC constraints

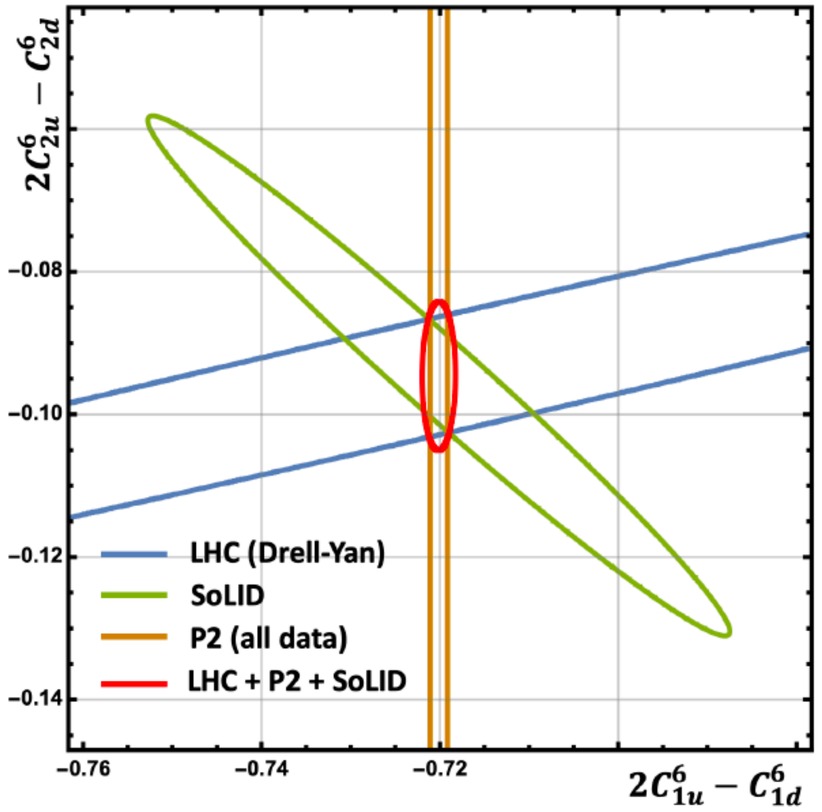

Boughezal, FP, Wiegand (2021)

Disentangling dim-6 and dim-8

- Both P2 and SoLID help remove degeneracies between dimension-6 and dimension-8 effects that appear when considering neutral-current Drell-Yan data at the LHC. A combined fit of both the high-energy and low-energy data is far more constraining than either data set independently.

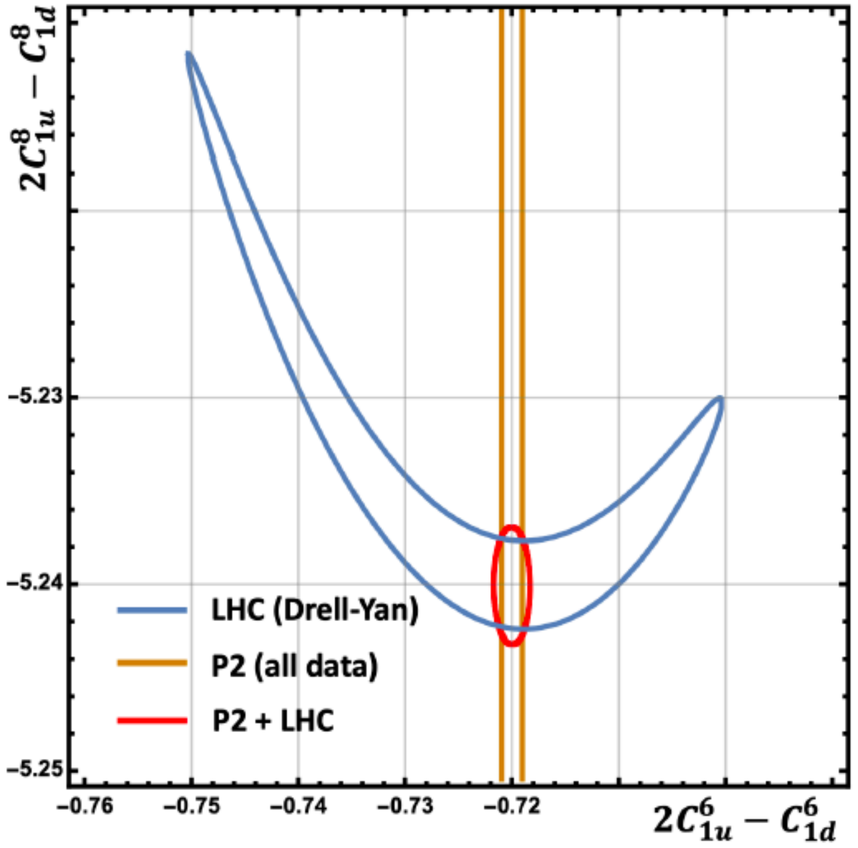

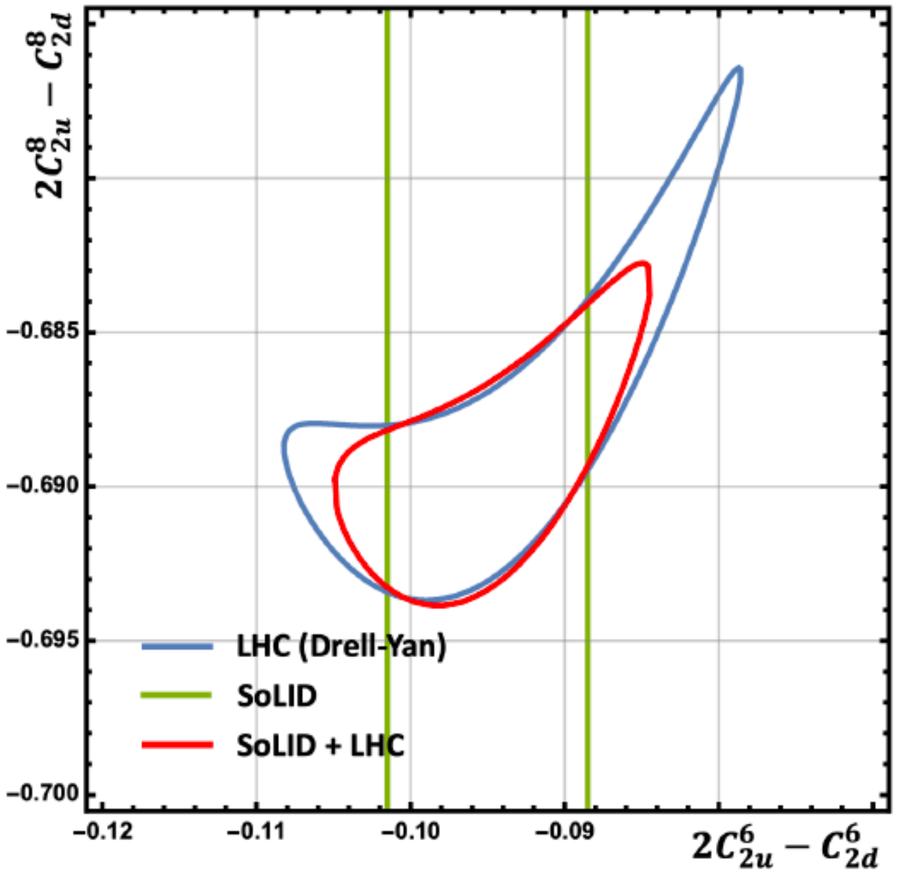

Boughezal, FP, Wiegand (2021)

Transverse spin asymmetries and anomalous dipole moments at the EIC

Boughezal, de Florian, FP, Vogelsang (2023)

Lepton anomalous magnetic moments

- One of the few measurements where there is a potential disagreement between the SM and experiments is the muon anomalous magnetic moment. The electron magnetic moment depends upon the fine structure constant. There is also a discrepancy between Cesium and Rubidium atomic recoil determinations of α, which lead to different electron magnetic moments.

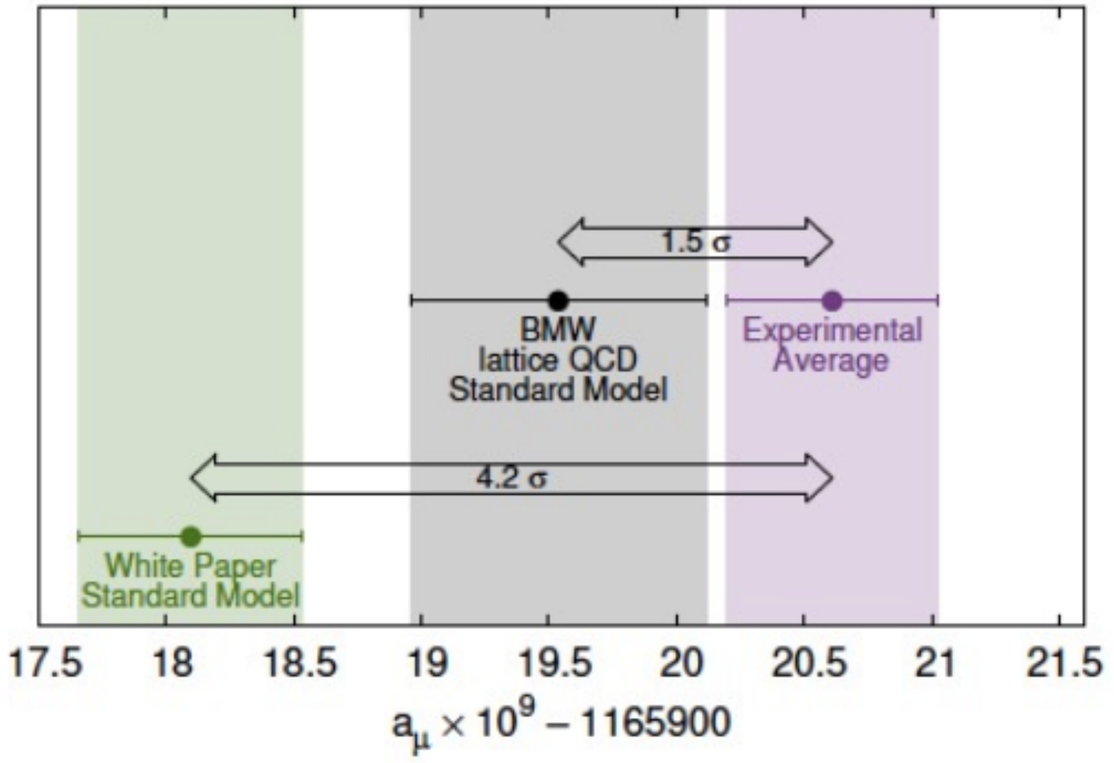

4σ discrepancy between the two determinations of Δa_e

$$\Delta a_e^{\mathrm{Cs}} = a_e^{\mathrm{exp}} - a_e^{\mathrm{SM,Cs}} = -0.88(36) \times 10^{-12}$$
$$\Delta a_e^{\mathrm{Rb}} = a_e^{\mathrm{exp}} - a_e^{\mathrm{SM,Rb}} = 0.48(30) \times 10^{-12}$$

Questions:

Could new physics explain the muon g-2 discrepancy? Can it shift the electron g-2 by a similar size as the observed discrepancy?

Lepton anomalous magnetic moments

- One of the few measurements where there is a potential disagreement between the SM and experiments is the muon anomalous magnetic moment. The electron magnetic moment depends upon the fine structure constant. There is also a discrepancy between Cesium and Rubidium atomic recoil determinations of α, which lead to different electron magnetic moments.

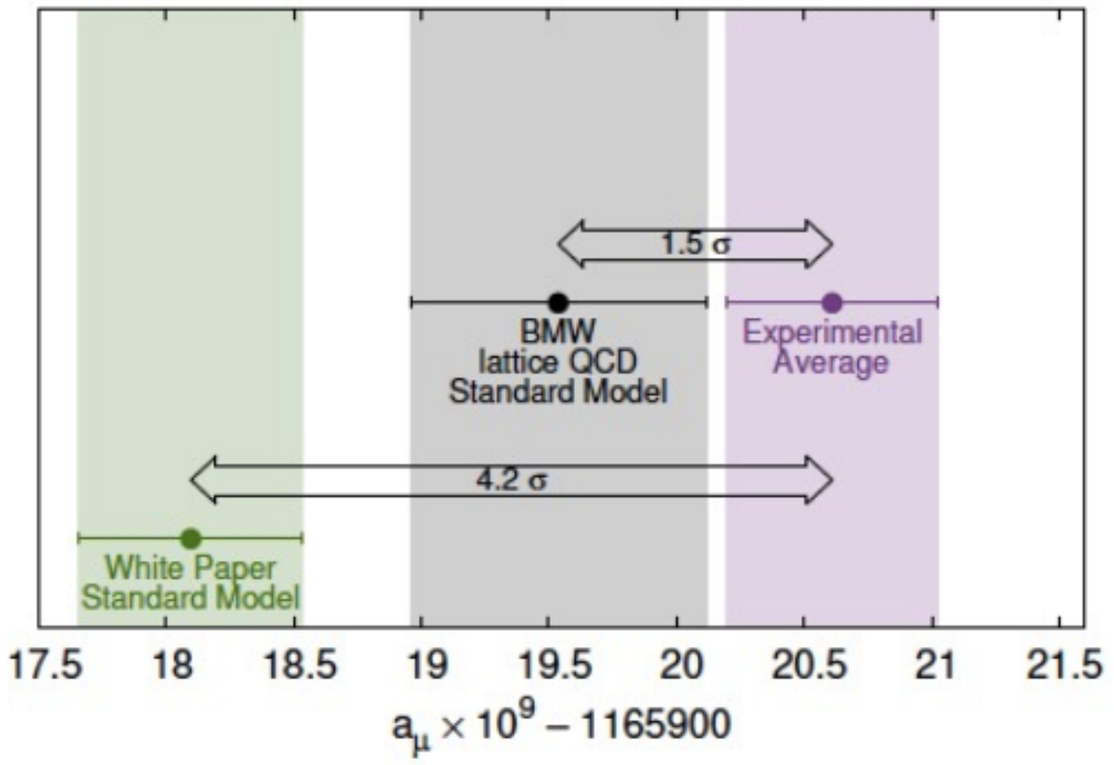

4σ discrepancy between the two determinations of Δa_e

$$\Delta a_e^{\rm Cs} = a_e^{\rm exp} - a_e^{\rm SM,Cs} = -0.88(36) \times 10^{-12}$$
$$\Delta a_e^{\rm Rb} = a_e^{\rm exp} - a_e^{\rm SM,Rb} = 0.48(30) \times 10^{-12}$$

In the SMEFT, beyond-the-SM contributions to the anomalous magnetic moments are described by the operators:

$$\mathcal{O}_{eW} = (\bar{l}_e \sigma^{\mu\nu} e)\tau^I \phi W^I_{\mu\nu}$$
$$\mathcal{O}_{eB} = (\bar{l}_e \sigma^{\mu\nu} e)\phi B_{\mu\nu}$$
$$\mathcal{O}_{\mu W} = (\bar{l}_\mu \sigma^{\mu\nu} \mu)\tau^I \phi W^I_{\mu\nu}$$
$$\mathcal{O}_{\mu B} = (\bar{l}_\mu \sigma^{\mu\nu} \mu)\phi B_{\mu\nu}$$

(real parts of Wilson coefficients for these operators give magnetic moments, imaginary parts give electric dipole moments)

Transverse SSAs at the EIC

- Another way to access these operators and probe the parameter space relevant for the lepton g-2 discrepancies is through transverse single-spin asymmetries at the Electron-Ion Collider.

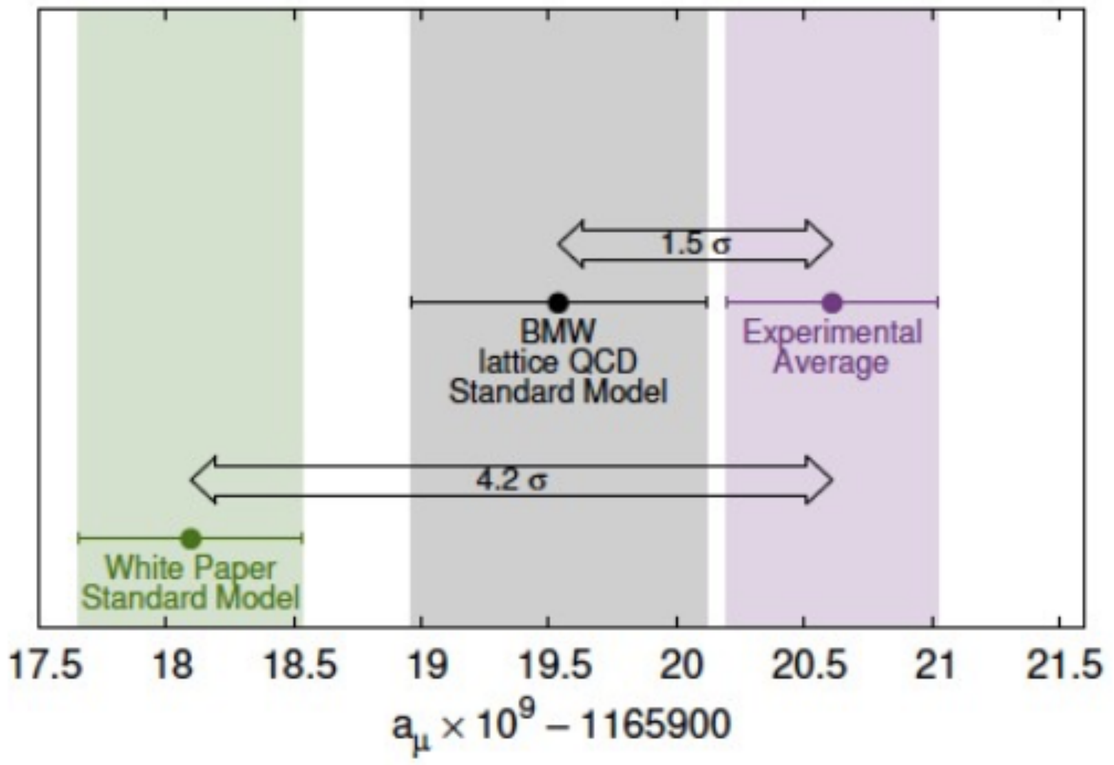

Transverse single-spin asymmetries are defined as the difference of cross sections for positive and negative polarization of a single beam, transverse to the beam direction. In the case of the electron being polarized we have

$$A_{TU} = \frac{\sigma(e^\uparrow) - \sigma(e^\downarrow)}{\sigma(e^\uparrow) + \sigma(e^\downarrow)}$$

Transverse polarization direction:

$$S_T^\mu = (0, \cos(\phi), \sin(\phi), 0)$$

Transverse SSAs in the SM

- There are two mechanisms that generate transverse SSAs in inclusive DIS in the SM. Historically the focus was on QED since these asymmetries were first considered at lower energies. One-photon exchange does not contribute due to the parity and time-reversal invariance of QED (Christ, Lee 1966) The leading mechanism is therefore two-photon exchange (Metz, Schlegel, Goeke 2006) :

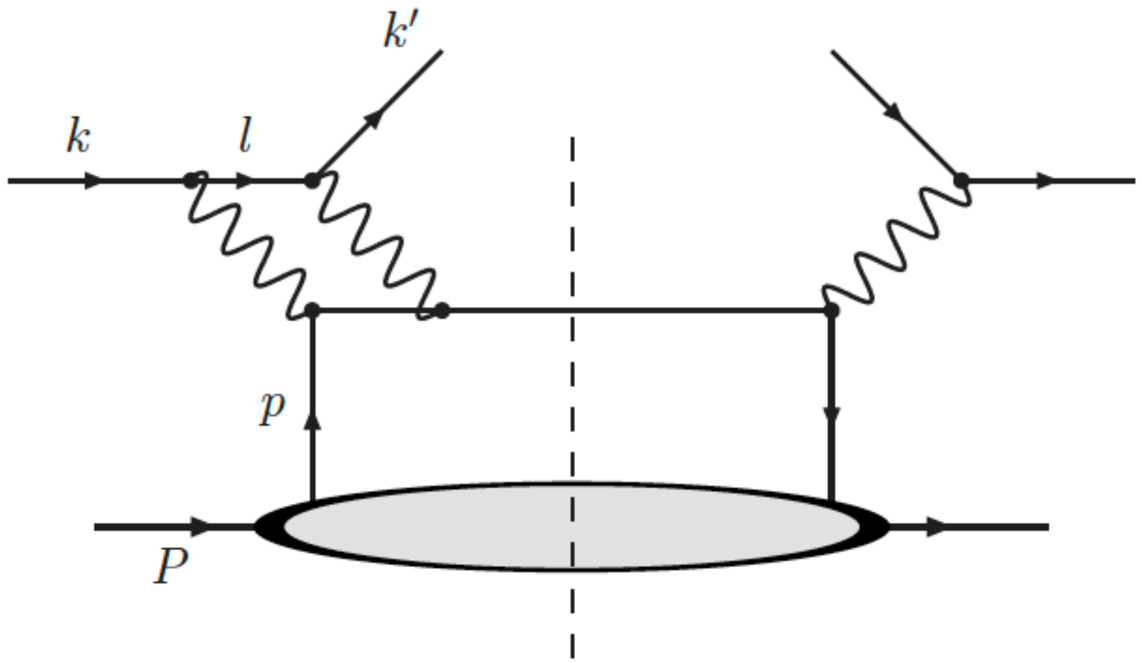

- Suppressed with respect to tree-level by a power of α
- Suppressed by the electron mass; easiest to see by studying the transverse projection operator:

$$u(p)\bar{u}(p) = \frac{1}{2}(\not{p} + m)(1 + \gamma_5 \not{S}_T)$$

  S_T changes number of gamma matrices from odd↔even

- "Naive" time-reversal invariant, and therefore requires the absorptive part of the one-loop amplitude

Transverse SSAs in the SM

- There are two mechanisms that generate transverse SSAs in inclusive DIS in the SM. Historically the focus was on QED since these asymmetries were first considered at lower energies. One-photon exchange does not contribute due to the parity and time-reversal invariance of QED (Christ, Lee 1966) The leading mechanism is therefore two-photon exchange (Metz, Schlegel, Goeke 2006) :

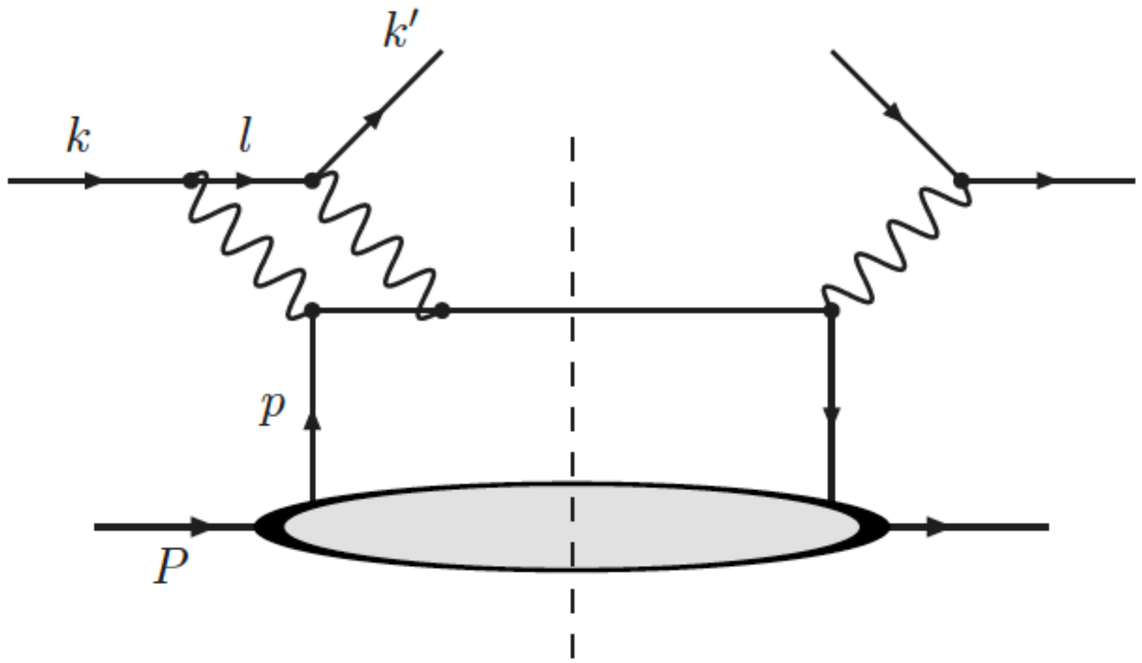

$$A_{TU}^{\gamma\gamma} = \alpha \frac{m_l}{2Q} \sin(\phi) \frac{y^2\sqrt{1-y}}{1-y+y^2/2} \frac{\sum_q Q_q^3 f_q(x)}{\sum_q Q_q^2 f_q(x)}$$

Doubly-suppressed by two small quantities

Depends on the transverse-plance azimuthal angle between the initial polarization and the final-state lepton

Transverse SSAs in the SM

- We pointed out that a second mechanism exists at high energies, Z-exchange, which will be important at a future EIC. (Boughezal, de Florian, FP, Vogelsang 2023)

$$A_{TU}^{Z}(\phi) = \frac{2}{s_W^2 c_W^2}\frac{m_l Q}{M_Z^2}\frac{y\sqrt{1-y}}{1-y+y^2/2}\cos(\phi)\frac{\sum_q Q_q f_q(x)\left[g_{al}g_{vq}(1-y)+g_{vl}g_{aq}y\right]}{\sum_q Q_q^2 f_q(x)}$$

Grows with momentum transfer

Different azimuthal angle dependence than photon contribution

Parity violating $g_v g_a$ dependence

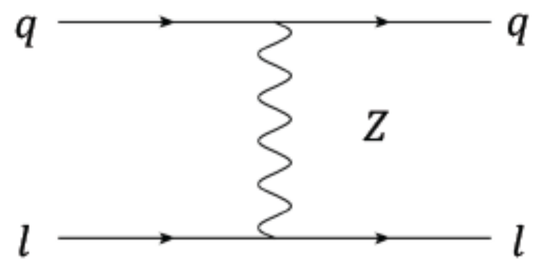

A_{TU}~10^{-6} in the SM; negligibly small and an excellent channel for new physics searches!

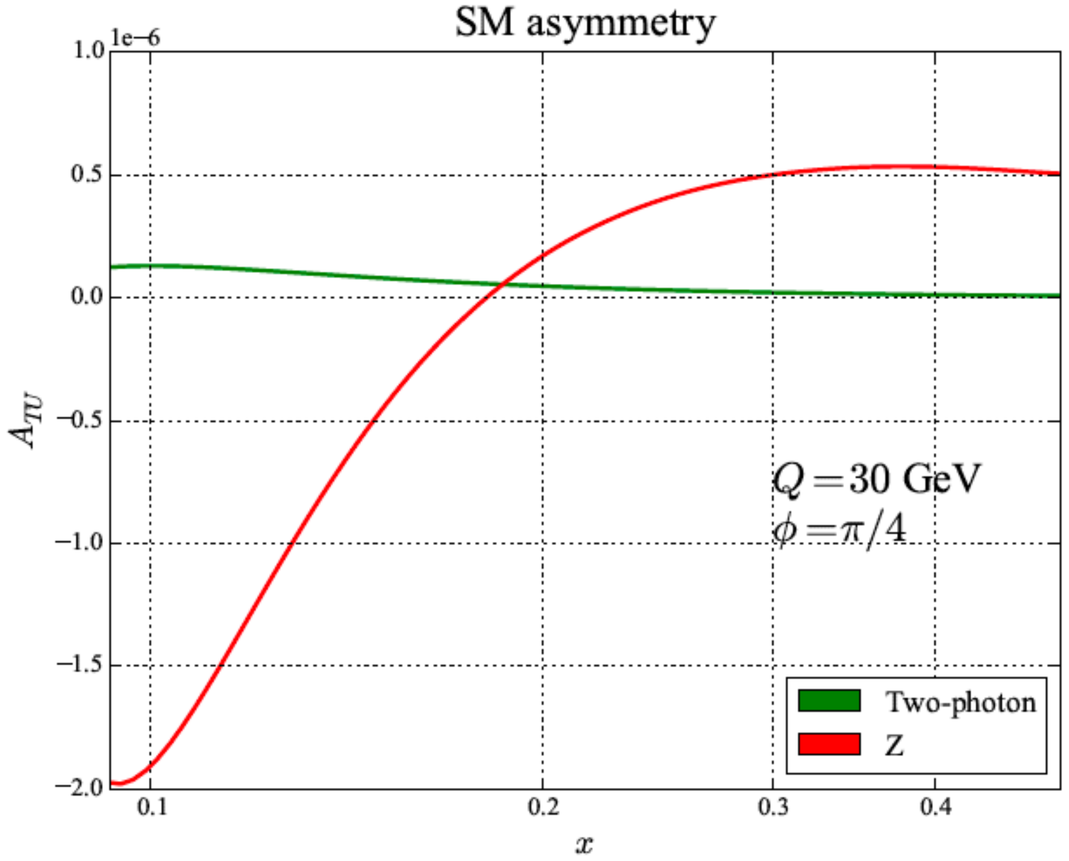

Transverse SSAs beyond the SM

- What kind of new physics can modify the transverse SSAs? We will focus on chiral operators, to avoid an explicit mass suppression factor. The new Wilson coefficients can of course contain this chiral suppression, but we expect them to already be small due to the mass gap between new physics and the SM. We don't want two small factors.

Scalar/tensor four-fermion operators

$$\mathcal{O}_{ledq} = (\bar{l}^j e)(\bar{d} q^j),$$
$$\mathcal{O}^{(1)}_{lequ} = (\bar{l}^j e)\epsilon_{jk}(\bar{q}^k u),$$
$$\mathcal{O}^{(3)}_{lequ} = (\bar{l}^j \sigma^{\mu\nu} e)\epsilon_{jk}(\bar{q}^k \sigma_{\mu\nu} u)$$

Scalar Higgs exchanges

$$\mathcal{O}_{e\varphi} = (\varphi^\dagger \varphi)(\bar{l} e \varphi),$$
$$\mathcal{O}_{u\varphi} = (\varphi^\dagger \varphi)(\bar{q} u \tilde{\varphi}),$$
$$\mathcal{O}_{d\varphi} = (\varphi^\dagger \varphi)(\bar{q} d \varphi).$$

Dipole operators

$$\mathcal{O}_{eW} = (\bar{l}\sigma^{\mu\nu} e)\tau^I \varphi W^I_{\mu\nu},$$
$$\mathcal{O}_{eB} = (\bar{l}\sigma^{\mu\nu} e)\varphi B_{\mu\nu},$$
$$\mathcal{O}_{uW} = (\bar{q}\sigma^{\mu\nu} u)\tau^I \varphi W^I_{\mu\nu},$$
$$\mathcal{O}_{uB} = (\bar{q}\sigma^{\mu\nu} u)\varphi B_{\mu\nu},$$
$$\mathcal{O}_{dW} = (\bar{q}\sigma^{\mu\nu} d)\tau^I \varphi W^I_{\mu\nu},$$
$$\mathcal{O}_{dB} = (\bar{q}\sigma^{\mu\nu} d)\varphi B_{\mu\nu}.$$

Explicit calculation shows that both four-fermion and Higgs operators require an explicit lepton mass insertion to contribute to transverse SSAs. This is true when dim-6 is interfered with the SM and when we consider dim-6 squared.

Dipole operators contribute when interfered with the SM. Transverse SSAs can isolate these same contributions that affect anomalous magnetic (and electric as we'll see) moments!

Structure of the SMEFT asymmetry

- The expression for the SMEFT asymmetry takes the form shown below.

$$C_{e\gamma} = \frac{v}{\sqrt{2}}\left[-s_W C_{eW} + c_W C_{eB}\right]$$
$$C_{eZ} = \frac{v}{\sqrt{2}}\left[-c_W C_{eW} - s_W C_{eB}\right]$$

$$\Delta A_{TU}(\phi) = \frac{g_Z}{2\pi\alpha}\frac{Q^3}{M_Z^2}\frac{y\sqrt{1-y}}{1-y+\frac{y^2}{2}}\frac{\sum_q Q_q f_q(x)\left\{g_{aq}\,\mathrm{Re}[C_{eZ}e^{-i\phi}] - \frac{\mathrm{Re}[C_{e\gamma}e^{-i\phi}]}{s_W c_W}\left[g_{vq}g_{al}(1-2/y) - g_{aq}g_{vl}\right]\right\}}{\sum_q Q_q^2 f_q(x)}$$

This asymmetry is sensitive to both the real and imaginary parts of the Wilson coefficients. The real part has a cos(φ) dependence, while the imaginary part has sin(φ).

Can extract them separately with appropriate weight functions:

$$A_{TU}^{w} = \int_0^{2\pi} d\phi\, w(\phi)\, A_{TU}(\phi)$$

w= cos(φ),sin(φ)

Sensitive to same operators as anomalous magnetic and electron dipole moments; can probe them separately; small SM background: an ideal new physics probe!

Numerics at an EIC

- The asymmetries range from 10^{-4} to 10^{-3} for moderate-to-high values of momentum transfers at an EIC, for TeV-scale new physics. The magnitudes for imaginary Wilson coefficients are similar. The expected errors at the EIC are roughly the same magnitude, indicating that an analysis binned in Q and x should probe TeV-scale new physics affecting dipole operators.

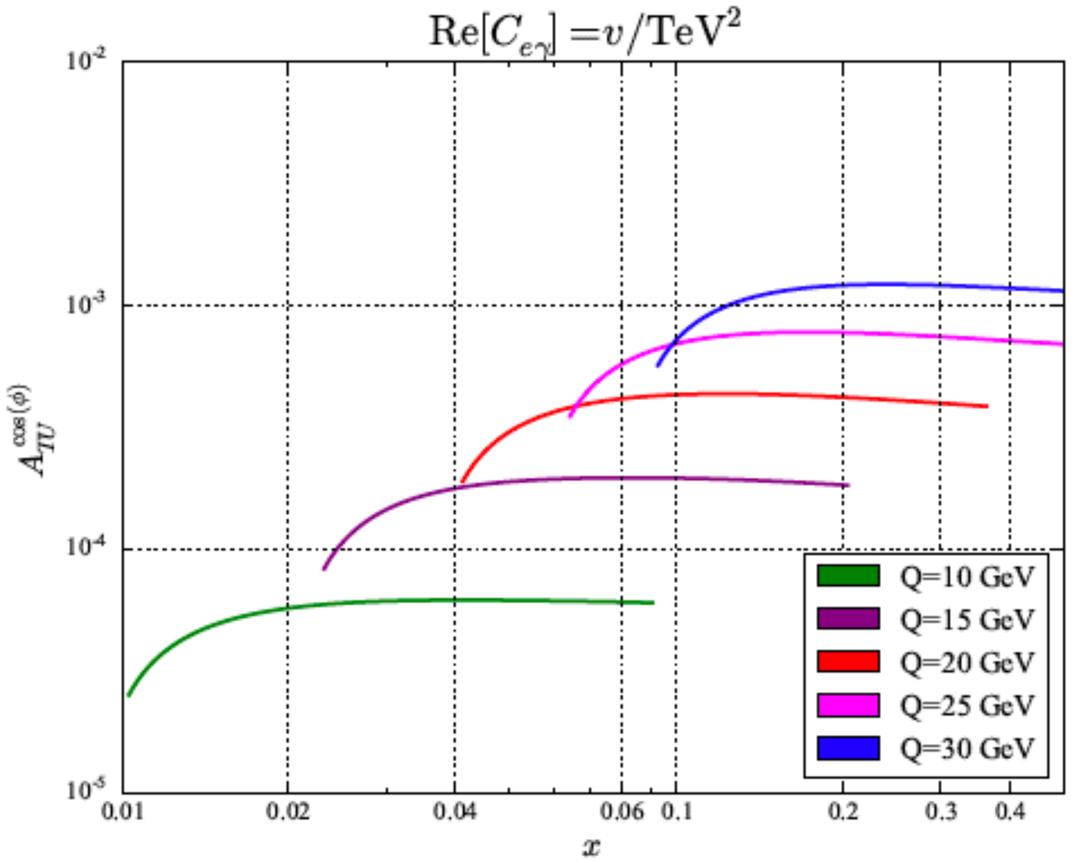

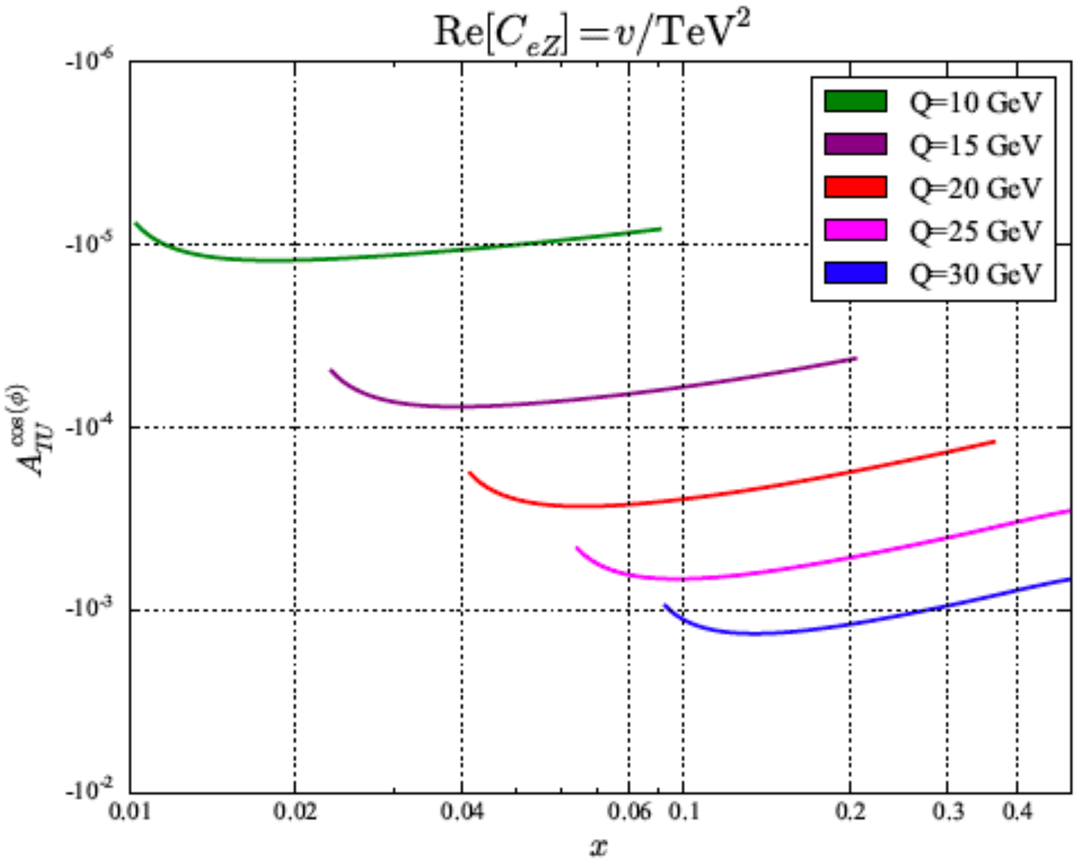

Complementarity with other probes

- In terms of the photon and Z dipole couplings, the electron anomalous magnetic moment can be written as follows. Note that only a single linear combination of the two parameters can be probed!

Aeibischer et al (2021)

$$(\Delta a_e)^{SMEFT} = \frac{m_e}{m_\mu}\left\{1.4\times 10^{-3} C_{e\gamma} - 1.3\times 10^{-5} C_{eZ}\right\}(250\,\mathrm{GeV})$$

$C_{e\gamma}$, C_{eZ} are MSbar parameters at the scale 250 GeV

- The low-energy theory below the EW scale contains only the photon dipole; C_{eZ} is generated by 1-loop running above the EW scale, hence the reduced sensitivity to this parameter
- The experiment-theory different is given by: $(\Delta a_e)^{exp-th} = \frac{m_e}{m_\mu}\begin{bmatrix} -1.8(7)^{\mathrm{Cs}} \\ 1.0(6)^{\mathrm{Rb}} \end{bmatrix} \times 10^{-10}$
- Assuming C_{ei}~vev/ Λ_{ei}^2, $C_{e\gamma}$ scales of O(100 TeV) are needed to explain the experiment-theory difference above; few-TeV C_{eZ} scales are needed.

Transverse SSAs at the EIC can help probe this parameter space in two ways: by measuring a separate linear combination of $C_{e\gamma}$, C_{eZ}, and by directly probing the C_{eZ} scales needed to address the discrepancy

A muon-ion collider

- A proposed upgrade of the EIC involves replacing the electron beam with a high-energy muon beam. This would provide the first step toward a high-energy muon-muon collider. Beam polarization reaching 50% are possible at such a machine (Acosta, Li 2021). Transverse SSAs at this machine would directly probe the couplings $C_{\mu\gamma}$, $C_{\mu Z}$ that address the muon g-2 discrepancy!

Machine parameters:

- 960 GeV muons x 275 GeV protons, for a CM energy around 1 TeV
- Assume 50% polarization, 50 fb^{-1} of integrated luminosity

Large asymmetries, greater than anticipated statistical errors. Scales of several TeV should be accessible at a muon-ion collider.

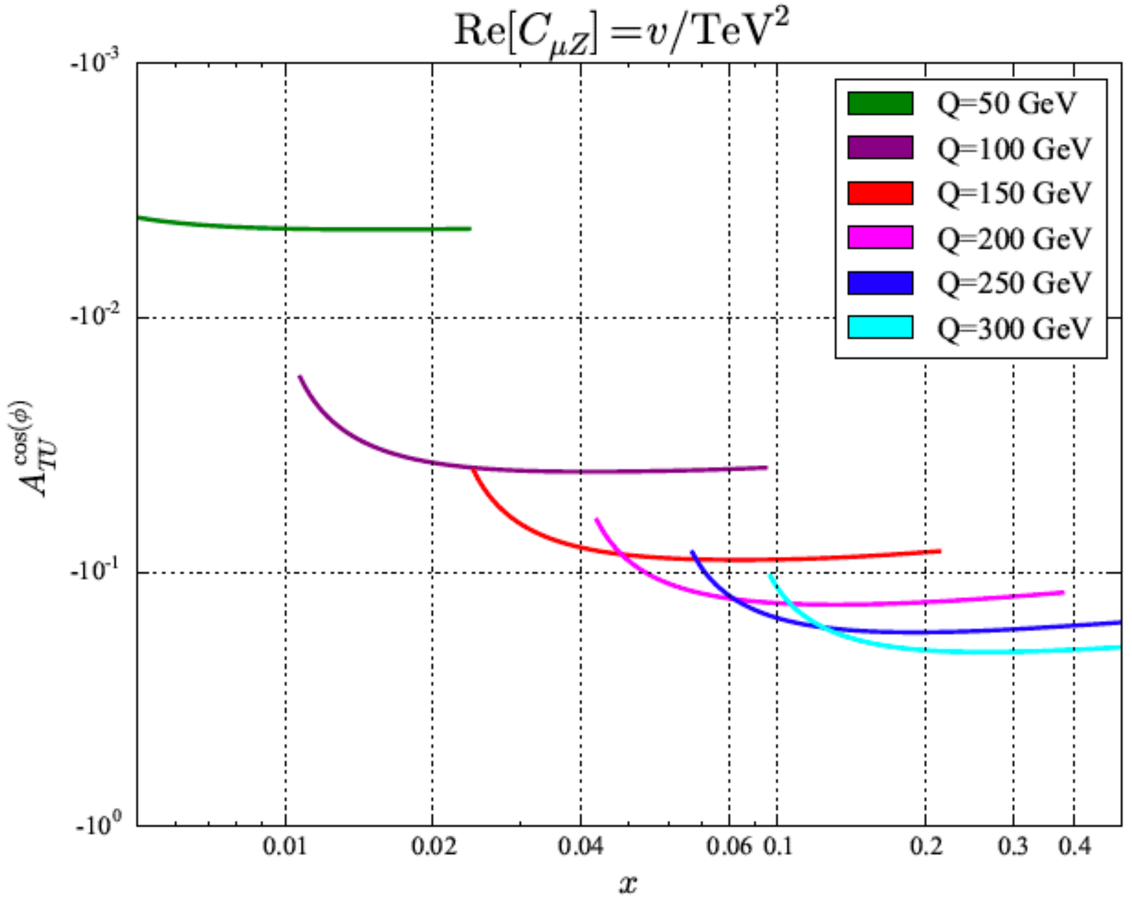

A muon-ion collider

- A proposed upgrade of the EIC involves replacing the electron beam with a high-energy muon beam. This would provide the first step toward a high-energy muon-muon collider. Beam polarization reaching 50% are possible at such a machine (Acosta, Li 2021). Transverse SSAs at this machine would directly probe the couplings $C_{\mu\gamma}$, $C_{\mu Z}$ that address the muon g-2 discrepancy!

$$\Delta a_\mu^{SMEFT} = 1.1 \times 10^{-3} \left(\frac{\mathrm{Re}[C_{\mu\gamma}]}{1\,\mathrm{TeV}^{-1}} \right) - 1.1 \times 10^{-5} \left(\frac{\mathrm{Re}[C_{\mu Z}]}{1\,\mathrm{TeV}^{-1}} \right)$$

$C_{e\gamma}$, C_{eZ} are now evaluated at 1 TeV

Aeibischer et al (2021)

- The experiment-theory different is given by: $\Delta a_\mu^{exp-SM} = 251(59) \times 10^{-11}$

The muon g-2 discrepancy can be explained, for example, by TeV-scale new physics for $C_{\mu\gamma} \approx 0.01 C_{\mu Z}$, which is a loop-factor suppression. Such a scenario is testable at the EIC

Transverse SSAs at a muon-ion collider can probe the same parameter space as the muon g-2!

The muon EDM

- So far we have focused on the real parts of the Wilson coefficients and the anomalous magnetic moments. Imaginary parts can be probed as well. They lead to CP-violating effects that also contribute to electric dipole moments. The electron EDM is too well constrained for the EIC to probe interesting parameter space, but the muon EDM is far less constrained.

$$\left|\frac{\Delta d_\mu}{d_\mu^{\rm exp}}\right| = 7.3 \times 10^2 \left(\frac{{\rm Im}[C_{\mu\gamma}]}{1\,{\rm TeV}^{-1}}\right) + 1.8 \left(\frac{{\rm Im}[C_{\mu Z}]}{1\,{\rm TeV}^{-1}}\right)$$

This gives the SMEFT-induced shift over the 90% CL experimental bound

Aeibischer et al (2021)

- Turning on only a single coefficient at a time, we find that Im[$C_{\mu\gamma}$] scales around 10 TeV can be probed by EDM measurements, above muon-ion collider capabilities
- However, only Im[$C_{\mu Z}$]~700 GeV can be probed with EDM measurements.

Transverse SSAs at a muon-ion collider can improve upon existing muon EDM constraints

Conclusions

- Although PVES and PVDIS experiments are lower energies than the LHC, their relatively high luminosity (with respect to previous DIS experiments such as HERA) and polarization provide unique handles on issues of interest to high energy physics.
- We've shown the PV asymmetry measurements at experiments P2, SoLID and the EIC play an important role in probing the SMEFT parameter space.
- We've shown here that transverse single-spin asymmetries at the EIC probe the same new physics parameter space as the muon and electron magnetic and electric dipole moment measurements.
- In particular a future muon-ion collider can improve upon existing muon EDM constraints, and can probe the new physics parameter space relevant for the muon g-2 anomaly.

Thank you!